Periostin in Cancer-Associated Fibroblasts Promotes Esophageal Squamous Cell Carcinoma Progression by Enhancing Cancer and Stromal Cell Migration

Miyako, Shoji ; Koma, Yu-ichiro ; Nakanishi, Takashi ; Tsukamoto, Shuichi ; Yamanaka, Keitaro ; Ishihara, Nobuaki ; Azumi, Yuki ;…

(Citation)
The American Journal of Pathology,194(5):828-848

(Issue Date)
2024-05

(Resource Type)
journal article

(Version)
Version of Record

(URL)
https://hdl.handle.net/20.500.14094/0100489205

The American Journal of Pathology, Vol. 194, No. 5, May 2024

ELSEVIER

The American Journal of
PATHOLOGY

ajp.amjpathol.org

TUMORIGENESIS AND NEOPLASTIC PROGRESSION

Periostin in Cancer-Associated Fibroblasts Promotes Esophageal Squamous Cell Carcinoma Progression by Enhancing Cancer and Stromal Cell Migration

Shoji Miyako,[*†] Yu-ichiro Koma,[*] Takashi Nakanishi,[*†] Shuichi Tsukamoto,[*] Keitaro Yamanaka,[*‡] Nobuaki Ishihara,[*§] Yuki Azumi,[*†] Satoshi Urakami,[*¶] Masaki Shimizu,[†] Takayuki Kodama,[*] Mari Nishio,[*] Manabu Shigeoka,[*] Yoshihiro Kakeji,[†] and Hiroshi Yokozaki[*]

From the Division of Pathology, Department of Pathology, the Divisions of Gastro-intestinal Surgery[†] and Hepato-Biliary-Pancreatic Surgery,[§] Department of Surgery, the Division of Obstetrics and Gynecology,[‡] Department of Surgery Related, and the Division of Gastroenterology,[¶] Department of Internal Medicine, Kobe University Graduate School of Medicine, Kobe, Japan*

Accepted for publication December 27, 2023.

Address correspondence to Yu-ichiro Koma, M.D., Ph.D., Division of Pathology, Department of Pathology, Kobe University Graduate School of Medicine, 7-5-1 Kusunoki-cho, Chuo-ku, Kobe 650-0017, Japan. E-mail: koma@med.kobe-u.ac.jp.

Cancer-associated fibroblasts (CAFs) in the tumor microenvironment are involved in the progression of various cancers, including esophageal squamous cell carcinoma (ESCC). CAF-like cells were generated through direct co-culture of human bone marrow–derived mesenchymal stem cells, one of CAF origins, with ESCC cells. Periostin (POSTN) was found to be highly expressed in CAF-like cells. After direct co-culture, ESCC cells showed increased malignant phenotypes, such as survival, growth, and migration, as well as increased phosphorylation of Akt and extracellular signal-regulated kinase (Erk). Recombinant human POSTN activated Akt and Erk signaling pathways in ESCC cells, enhancing survival and migration. The suppression of POSTN in CAF-like cells by siRNA during direct co-culture also suppressed enhanced survival and migration in ESCC cells. In ESCC cells, knockdown of POSTN receptor integrin β4 inhibited Akt and Erk phosphorylation, and survival and migration increased by POSTN. POSTN also enhanced mesenchymal stem cell and macrophage migration and endowed macrophages with tumor-associated macrophage–like properties. Immunohistochemistry showed that high POSTN expression in the cancer stroma was significantly associated with tumor invasion depth, lymphatic and blood vessel invasion, higher pathologic stage, CAF marker expression, and infiltrating tumor-associated macrophage numbers. Moreover, patients with ESCC with high POSTN expression exhibited poor postoperative outcomes. Thus, CAF-secreted POSTN contributed to tumor microenvironment development. These results indicate that POSTN may be a novel therapeutic target for ESCC. *(Am J Pathol 2024, 194: 828–848; https://doi.org/10.1016/j.ajpath.2023.12.010)*

Esophageal cancer is the seventh most common cancer worldwide and the sixth leading cause of cancer-related death.[1] The histologic types of esophageal cancer are broadly classified into esophageal squamous cell carcinoma (ESCC) and esophageal adenocarcinoma, with ESCC accounting for approximately 90% of esophageal cancers, especially in East Asia.[2,3] In East Asia and East Africa, esophageal cancer is one of the top five causes of overall cancer mortality, and the 5-year overall survival (OS) of ESCC is approximately 20%, with a poor prognosis.[1,4] The poor prognosis of patients with esophageal cancer is associated with a high propensity for metastasis, even if the tumor is superficial, as well as the fact that early esophageal cancer is often asymptomatic and tends to be diagnosed at an advanced stage.[2,5,6] Therefore, further investigation of the mechanisms of esophageal cancer development and progression is an urgent and unmet need.

The tumor microenvironment (TME), consisting of cancer cells, stromal cells, and extracellular matrix, is an essential factor affecting cancer progression; the TME

Supported by Japan Society for the Promotion of Science Grants-in-Aid for Scientific Research 20K07373 (H.Y.) and 22K06978 (Y.-i.K.); and Takeda Science Foundation grant (Y.-i.K.).

https://doi.org/10.1016/j.ajpath.2023.12.010

regulates cell proliferation, determines metastatic potential, decides the site of metastasis, and impacts therapeutic outcomes.[7,8] Cancer-associated fibroblasts (CAFs) are a major component of the TME and have diverse functions, including extracellular matrix deposition and remodeling, extensive signaling interactions with cancer cells, and crosstalk with infiltrating leukocytes, including macrophages.[9] A previous study showed that patients with ESCC with high amounts of CAFs expressing fibroblast activation protein (FAP) have a poor prognosis.[10] Yeo et al[11] also reported that Twist 1 expression in CAFs in ESCC was positively associated with depth of tumor invasion, lymph node metastasis, and advanced clinical stage and was a significant poor prognostic factor for OS. Furthermore, CAF marker expression could be a prognostic factor for patients with ESCC receiving neoadjuvant chemotherapy.[12]

Previous studies established an indirect co-culture system between ESCC cell lines and human mesenchymal stem cells (MSCs), one of CAF origins, to investigate the biological mechanisms of ESCC progression using CAFs. IL-6, C-C motif chemokine 2, and serine protease inhibitor E1 (SERPINE1), derived from CAF-like cells, generated via the indirect co-culture system promoted ESCC cell and macrophage migration.[10,13] Metallothionein 2A (MT2A) expressed in the same CAF-like cells also promoted the growth, migration, and invasion of ESCC cells.[14]

In the present study, a direct co-culture system of ESCC cell lines and MSCs was established to further elucidate the mechanism of ESCC progression induced by CAFs. Then, cDNA microarray analysis of mono-cultured MSCs and directly co-cultured CAF-like cells was performed, and the results were compared with those of indirectly co-cultured cells. Then, genes with higher expression in the direct co-cultured cells were identified, along with key factors that may provide new therapeutic targets and prognostic factors for ESCC.

Materials and Methods

Cell Lines and Cell Cultures

Three human ESCC cell lines (TE-9, TE-10, and TE-15) were obtained from the RIKEN BioResource Center (Tsukuba, Japan) and maintained in RPMI 1640 medium (Wako, Osaka, Japan) with 10% fetal bovine serum (FBS; Sigma-Aldrich, St. Louis, MO) and 1% antibiotic-antimycotic (Invitrogen, Carlsbad, CA).[13,15] Human bone marrow–derived MSCs were purchased from the ATCC (PCS-500-012; Manassas, VA) and maintained in low-glucose Dulbecco's modified Eagle's medium (Wako) with 10% FBS and 1% antibiotic-antimycotic.[10,13,14] CD14-positive peripheral blood monocytes were collected from the peripheral blood of healthy volunteers via positive selection using the autoMACS Pro Separator (Miltenyi Biotec, Bergisch Gladbach, Germany). In brief, after isolation using anti-CD14 microbeads (130-050-201; Miltenyi Biotec), peripheral blood monocytes were seeded into 6-well plates (5×10^5 cells per well) and cultured in RPMI 1640 medium containing 10% FBS and cultured with recombinant human macrophage colony-stimulating factor (10 ng/mL; R&D Systems, Minneapolis, MN) and recombinant human granulocyte-macrophage colony-stimulating factor (1 ng/mL; R&D Systems) for 6 days to induce macrophage polarity.[16] All cells were cultured in a humidified atmosphere at 37°C and 5% CO_2.

Direct Co-Culture System

To induce the CAF-like cells, 3×10^5 MSCs were seeded into a 100-mm dish, and 2×10^5 TE cells were seeded in the same dish after 3 hours. Direct co-culture was performed for 4 days in high-glucose Dulbecco's modified Eagle's medium (Wako) with 10% FBS and 1% antibiotic-antimycotic. MSCs and TE cells were seeded and cultured similarly without co-culture as controls. Following direct co-culture, the dishes were washed three times with phosphate-buffered saline (PBS; Wako), the cells were trypsinized to form a single-cell suspension, and the reaction was stopped with a trypsin inhibitor (Sigma-Aldrich). Cell suspensions were mixed with anti-CD326 [epithelial cell adhesion molecule (EpCAM)] microbeads (number 130-061-101; Miltenyi Biotec) and incubated at 4°C for 30 minutes. The prepared cell suspensions were separated from EpCAM-positive and EpCAM-negative cells using an autoMACS Pro Separator (Miltenyi Biotec). Mono-cultured TE cells and MSCs were collected using an autoMACS Pro Separator, similar to direct co-culture cells (Figure 1A).

cDNA Microarray Analysis

Total RNA extraction from mono-cultured MSCs and MSCs directly co-cultured with TE-9 cells was performed using the RNeasy Mini Kit (Qiagen, Hilden, Germany). The cDNA microarray was analyzed using a 3D-Gene Human Oligo Chip 25k (Toray Industries, Tokyo, Japan). Microarray slides were scanned using 3D-Gene Scanner (Toray Industries) and processed using 3D-Gene Extraction software (Toray Industries). The obtained data were registered in the Gene Expression Omnibus database (*http://www.ncbi.nlm.nih.gov/geo*; accession number GSE244020). The present study also used the cDNA microarray analysis results from indirect co-cultures of MSCs and TE cells established in a previous study,[13] deposited in the Gene Expression Omnibus database (*http://www.ncbi.nlm.nih.gov/geo*; accession number GSE143138).

RT-PCR and qPCR

Total RNA was extracted from cells using the RNeasy Mini Kit (Qiagen), according to the manufacturer's instructions, and quantified using NanoDrop Lite (Thermo Fisher Scientific, Waltham, MA). The RT-PCR products of EpCAM,

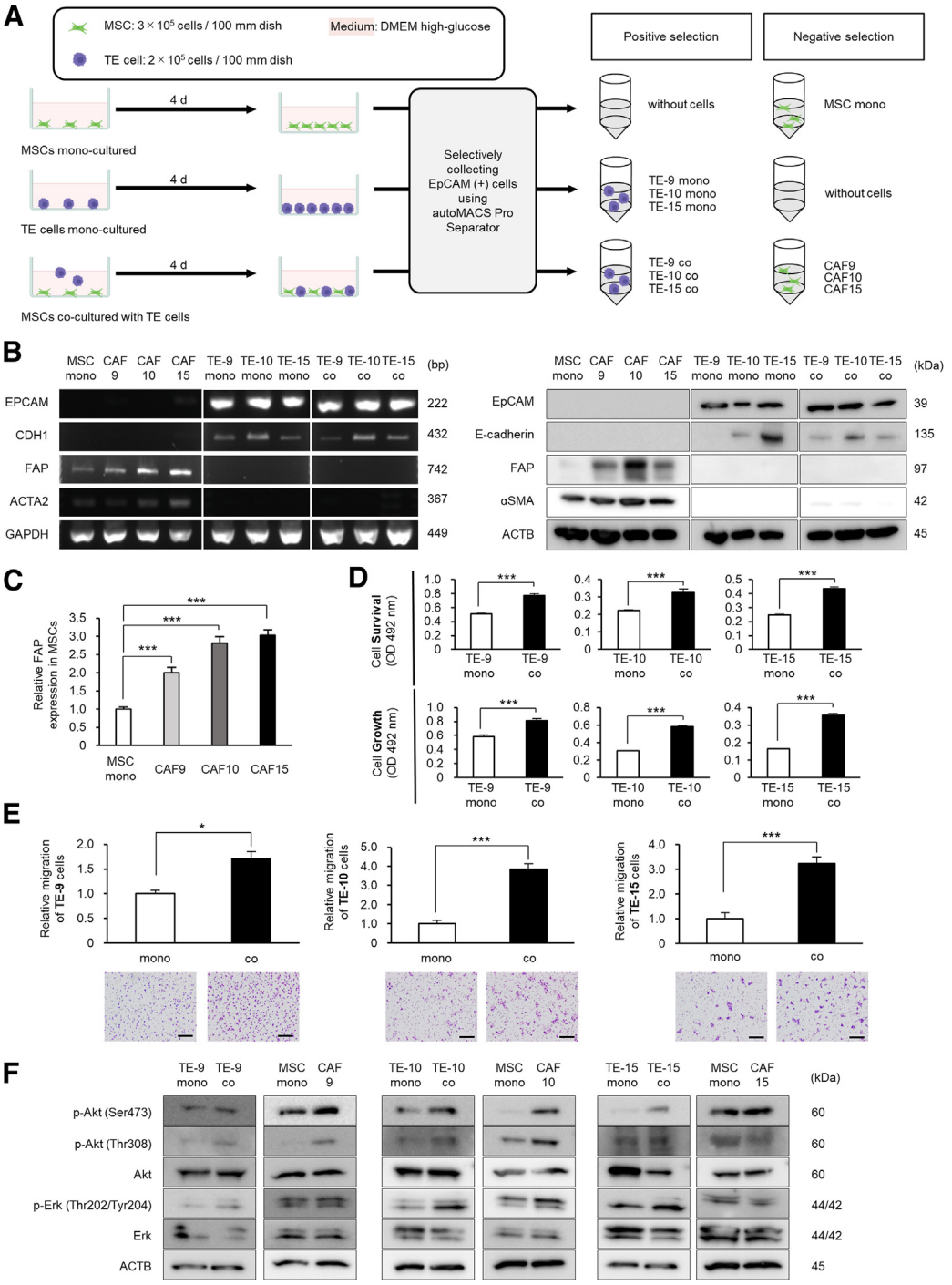

Figure 1 Esophageal squamous cell carcinoma (ESCC) cells exhibit enhanced survival, growth, and migration after direct co-culture with mesenchymal stem cells (MSCs). **A:** Direct co-culture of ESCC cell lines (TE-9, TE-10, and TE-15) and MSCs was performed for 4 days. MSCs and TE cells were seeded similarly without co-culture and cultured for 4 days as mono-cultured controls. After direct co-culture, epithelial cell adhesion molecule (EpCAM)—positive (TE-9 co, TE-10 co, and TE-15 co) and EpCAM-negative cells [cancer-associated fibroblast (CAF) 9, CAF10, and CAF15] were separated through magnetic-activated cell sorting (MACS). Mono-cultured MSCs (MSC mono) and mono-cultured TE cells (TE-9 mono, TE-10 mono, and TE-15 mono) were passed through MACS as controls. **B:** In each cell after separation using MACS, RT-PCR confirmed the expression of EPCAM, cadherin 1 (CDH1), fibroblast activation protein (FAP), and actin alpha 2 (ACTA2) (**left panel**), and Western blot analysis confirmed the expression of EpCAM, E-cadherin, FAP, and α-smooth muscle actin (α-SMA) (**right panel**). Glyceraldehyde-3-phosphate dehydrogenase (GAPDH) and beta actin (ACTB) were used as controls in RT-PCR and Western blot analysis, respectively. **C:** FAP expression in CAF9, CAF10, and CAF15 was compared with that in MSCs using real-time quantitative PCR. **D:** MTS assays were performed between TE cells after mono-culture and direct co-culture to evaluate the survival and growth of TE cells. **E:** Transwell migration assays were performed between TE cells after mono-culture and direct co-culture. Migrating cells were counted in five random fields in each chamber after 48 hours of incubation. Typical images are shown below. **F:** Western blot analysis of Akt, phosphorylated Akt (p-Akt; Ser473), p-Akt (Thr308), extracellular signal-regulated kinase (Erk), and phosphorylated Erk (p-Erk; Thr202/Tyr204) in mono-cultured and co-cultured TE-9, TE-10, TE-15 cells and MSC mono, CAF9, CAF10, and CAF15. ACTB was used as a control. Data are presented as means ± SEM (**C**—**E**). $*P < 0.05$, $***P < 0.001$. Scale bars = 100 μm (**E**).

cadherin 1 (CDH1), FAP, actin alpha 2 (ACTA2), integrin subunit beta 4 (ITGB4), and glyceraldehyde-3-phosphate dehydrogenase (GAPDH; control) were separated using 2% agarose gel electrophoresis. The quantitative real-time PCR (qPCR) for periostin (POSTN), ITGB4, CD163, CD204, IL-10, IL-12, and GAPDH was performed using SYBR Green PCR Master Mix (Applied Biosystems, Foster City, CA). For FAP, ACTA2, IL-6, MT2A, SERPINE1, and beta actin (ACTB), it was performed using TaqMan Gene Expression Master Mix (Applied Biosystems) on the ABI StepOne Real-Time PCR System (Applied Biosystems). The C_T values were evaluated by plotting the observed fluorescence against the number of cycles and analyzed using the comparative C_T method. The values were normalized against those of GAPDH for SYBR Green PCR Master Mix and against those of ACTB for TaqMan Gene Expression Master Mix. Relative gene expression was calculated as follows: relative expression $= 2^{-[C_T \text{ (target gene)} - C_T \text{ (GAPDH)}]}$. The following primers were used for RT-PCR: EPCAM, 5′-ATTTGCTCAAAGCTGGCTGC-3′ (forward) and 5′-AGTGTCCTTGTCTGTTCTTCTGACC-3′ (reverse); CDH1, 5′-CCTTCCTCCCAATACATATCCC-3′ (forward) and 5′-TCTCCGCCTTCTTCATC-3′ (reverse); FAP, 5′-GTTATTGCCTATTCCTATTATG-3′ (forward) and 5′-GTCCATCATGAAGGGTGGAAA-3′ (reverse); ACTA2, 5′-ACGATGCTCCCAGGGCTG-3′ (forward) and 5′-GAGAGACAGCACCGCCTGG-3′ (reverse); ITGB4, 5′-GCTTCACACCTATTTCCCTGTC-3′ (forward) and 5′-GACCCAGTCCTCGTCTTCTG-3′ (reverse); and GAPDH, 5′-GTCAGTGGTGGACCTGACCT-3′ (forward) and 5′-TGTGAGGAGGGGAGATTCAG-3′ (reverse). For qPCR using SYBR Green PCR Master Mix, the following primer were used: POSTN, 5′-CAACGGGCAAATACTGGAAAC-3′ (forward) and 5′-TCTCGCGGAATATGTGAATCG-3′ (reverse); ITGB4, 5′-GCTTCACACCTATTTCCCTGTC-3′ (forward) and 5′-GACCCAGTCCTCGTCTTCTG-3′ (reverse); CD163, 5′-CGAGTTAACGCCAGTAAG-3′ (forward) and 5′-GAACATGTCACGCCAGC-3′ (reverse); CD204, 5′-CCAGGGACATGGGAATGCAA-3′ (forward) and 5′-CCAGTGGGACCTCGATCTCC-3′ (reverse); IL-10, 5′-GGTTGCCAAGCCTTGTCTGA-3′ (forward) and 5′-AGGGAGTTCACATGCGCCT-3′ (reverse); IL-12, 5′-GCTGGCAGTTATTGATGAGC-3′ (forward) and 5′-GCATGAAGAAGTATGCAGAGC-3′ (reverse); and GAPDH, 5′-GCACCGTCAAGCCTGAGAAT-3′ (forward) and 5′-ATGGTGGTCAAGACGCCAGT-3′ (reverse). The following probes were used for qPCR using TaqMan Gene Expression Master Mix: FAP, Hs00990806_m1; ACTA2, Hs00426835_g1; IL-6, Hs00174131_m1; MT2A, Hs02379661_g1; SERPINE1, Hs00167155_m1; and ACTB, Hs01060665_g1.

Western Blot Analysis

Cells were lysed on ice with RIPA Lysis and Extraction Buffer (Thermo Fisher Scientific) containing 1% protease inhibitor and 1% phosphatase inhibitor cocktails (Sigma-Aldrich). After lysis, proteins were quickly collected via centrifugation, and concentrations were measured using NanoDrop Lite (Thermo Fisher Scientific). The resulting lysates were separated onto 5% to 20% SDS polyacrylamide gels and transferred to a membrane with an iBlot2 Gel Transfer Stack (Invitrogen). Membranes were blocked with 5% skim milk at room temperature for 30 minutes and incubated overnight with primary antibodies at 4°C. Then, they were washed three times with tris-buffered saline containing 0.1% Tween-20 (Thermo Fisher Scientific) and incubated with the secondary antibodies for 90 minutes at room temperature. After washing three times with tris-buffered saline containing 0.1% Tween-20, the protein bands were detected with ImmunoStar Reagents (Wako). In some experiments, TE-9, TE-10, and TE-15 cells in serum-free RPMI 1640 medium were treated with recombinant human periostin (rhPOSTN; 100 pg/mL; number 3548-F2; R&D Systems) for 0, 10, 30, and 60 minutes before lysis. The bands were quantified using the wand (tracing) tool in ImageJ software version 1.54f (NIH, Bethesda, MD; *https://imagej.nih.gov/ij*).

All antibodies were obtained from Cell Signaling Technology (Danvers, MA), unless otherwise indicated. The primary antibodies were as follows: mouse antibody against EpCAM (1:100; number 2929); rabbit antibody against E-cadherin (1:100; number 3159); sheep antibody against FAP (1:300; number AF3715; R&D Systems); rabbit antibody against α-smooth muscle actin (1:300; number ab5694; Sigma-Aldrich); rabbit antibody against phosphorylated Akt (p-Akt; Ser473; 1:100; number 4060); rabbit antibody against phosphorylated Akt (Thr308; 1:100; number 2965); rabbit antibody against Akt (1:100; number 9272); rabbit antibody against phosphorylated extracellular signal-regulated kinase (Erk; Thr202/Tyr204; 1:100; number 9101); rabbit antibody against Erk (1:100; number 9102); rabbit antibody against integrin β4 (1:200; number 14803); mouse antibody against CD163 (1:100; number NCL-L-CD163; Leica Biosystems, Wetzlar, Germany); mouse antibody against CD204 (1:200; number KT022; Trans Genic, Kobe, Japan); and rabbit antibody against ACTB (1:2000; number 4970). The secondary antibodies were as follows: horseradish peroxidase–conjugated donkey anti-rabbit IgG (1:1000; number NA934V; Cytiva, Marlborough, MA); sheep anti-mouse IgG (1:1000; number NA931V; Cytiva); and donkey anti-sheep IgG (1:1000; number ab6900; Abcam, Cambridge, UK).

Enzyme-Linked Immunosorbent Assay

Mono-cultured MSCs and MSCs directly co-cultured with TE-9, TE-10, and TE-15 cells (defined as CAF9, CAF10, and CAF15, respectively) were incubated in 6-well plates (2×10^5 cells per well) with 3 mL of low-glucose Dulbecco's modified Eagle's medium (Wako) containing 10% FBS. After 48 hours of incubation, the supernatants were

collected and analyzed using Human Periostin/OSF-2 DuoSet ELISA (R&D Systems), according to the manufacturer's instructions. The ODs of each well were read at 450- and 570-nm wavelengths using a Microplate Reader Infinite 200 PRO (Tecan, Mannedorf, Switzerland). The concentrations of each well were calculated from the measured absorbance using a standard curve.

Knockdown of *POSTN* and *ITGB4* in Direct Co-Culture System and ESCC Cell Lines

For *POSTN* knockdown, the direct co-culture system, including TE-9, TE-10, or TE-15 cells and MSCs, was transfected with siRNA targeting human *POSTN* (20 pmol; sc-61324; Santa Cruz Biotechnology, Dallas, TX) using Lipofectamine RNAiMAX (Invitrogen) for 96 hours, according to the manufacturer's instructions. After direct co-culture with siRNA, co-cultured TE cells and MSCs were separated as described in *Direct Co-Culture System*. For *ITGB4* knockdown, TE-9, TE-10, and TE-15 cells were transfected with siRNA targeting human *ITGB4* (20 pmol; sc-35678; Santa Cruz Biotechnology) using Lipofectamine RNAiMAX (Invitrogen) for 48 hours, according to the manufacturer's instructions. MISSION siRNA Universal Negative Control #1 (20 pmol; Sigma-Aldrich) was used as a negative control in both experiments. After transfection, cells were used for *in vitro* experiments.

Cell Survival and Growth Assay (MTS Assay)

Cells were seeded on 96-well plates at 1×10^4 per well with serum-free RPMI 1640 medium for the cell survival assay or at 5×10^3 per well with 1% FBS for the cell growth assay, followed by incubation at 37°C. CellTiter 96 Aqueous One Solution Reagent (Promega, Madison, WI) was applied after 48 hours. The absorbance was measured using a microplate reader (Infinite 200 PRO; Tecan) at 492 nm. In some experiments, rhPOSTN (100 pg/μL) was added to the culture medium when cells were seeded into 96-well plates.

Transwell Migration Assay

Transwell migration assays were performed using an 8.0-μm pore size insert (Falcon, BD, Franklin Lakes, NJ) as the upper chamber and 24-well plates as the lower chamber. TE-9, TE-10, or TE-15 cells were seeded in the upper chambers (1×10^5 cells per well), with 300 μL serum-free RPMI 1640 medium. The upper chambers were exposed to the lower chambers with 800 μL RPMI 1640 medium containing 0.1% FBS. After 48 hours of incubation at 37°C in 5% CO_2, the cells on the upper chamber were fixed with methanol for 1.5 minutes and stained with Diff-Quik (Sysmex, Kobe, Japan). After three washes with milli-Q water (Millipore, Bedford, MA), adherent cells on the upper surface of the membrane in the upper chamber were gently removed with cotton swabs. Cells migrating onto the lower surface of the membrane were counted in five random fields on each surface, and images were obtained at ×100 magnification using a charge-coupled device camera (Olympus, Tokyo, Japan). In some experiments, rhPOSTN (100 pg/μL) with or without phosphatidylinositol 3-kinase (PI3K) inhibitor (LY294002; 10 μmol/L; Cell Signaling Technology) or MEK1/2 inhibitor (PD98059; 10 μmol/L; Cell Signaling Technology) was added into the lower chambers.

Wound Healing Assay

TE-9 and TE-10 cells were seeded in 24-well plates (2×10^5 cells per well) with 600 μL of RPMI 1640 medium containing 10% FBS and incubated at 37°C in 5% CO_2 for 24 hours. The confluent cell monolayers were scratched in a straight line with a 1000-μL pipette tip. After three washes with PBS, four scratch fields in each well were captured using a charge-coupled device camera at ×40 magnification. The medium was then replaced with 600 μL of serum-free RPMI 1640 medium with or without rhPOSTN (100 pg/mL) and incubated at 37°C in 5% CO_2 for 24 hours. Each well was washed three times with PBS, and cells migrating to the wound area were captured similarly. To assess the range of migration, percentage wound coverage was calculated using the polygon selection tool in ImageJ software version 1.54f.

Immunofluorescence

Peripheral blood monocytes were collected as described in *Cell Lines and Cell Cultures* and seeded (5×10^4 cells) in Lab-Tek II 4-well chamber slides (Thermo Fisher Scientific) with 1 mL of RPMI 1640 medium containing 10% FBS, recombinant human macrophage colony-stimulating factor (10 ng/mL), and recombinant human granulocyte-macrophage colony-stimulating factor (1 ng/mL) for 6 days for macrophage differentiation. Following differentiation, the chambers were washed three times with PBS (Wako) and treated with 1 mL of serum-free RPMI 1640 medium with or without rhPOSTN (100 pg/mL) for 2 days. Cells were then fixed with 4% paraformaldehyde (Wako) for 10 minutes at room temperature and incubated with anti-CD163 (1:200; number NCL-L-CD163; Leica Biosystems) or anti-CD204 (1:200; number KT022; Trans Genic) primary antibody at 4°C overnight. Then, cells were washed and incubated at room temperature for 60 minutes with Cy3-conjugated anti-mouse IgG (1:200; Jackson ImmunoResearch Laboratories, West Grove, PA) secondary antibody and DAPI (1:1000; Wako). Slides were washed three times with PBS, and images were obtained by the BX50 fluorescence microscope using DP73 digital camera with cellSens Standard 1.6 software (Olympus). Then, the percentage of CD163-and CD204-positive cells among the total number of DAPI-positive cells was evaluated using

TissueQuest software version 4.0 (TissueGnotics, Vienna, Austria), as previously reported.[17]

Tissue Samples

Tissue samples were collected from patients who underwent surgical resection of human ESCC between 2005 and 2010 at Kobe University Hospital (Kobe, Japan). Patients who received preoperative adjuvant chemotherapy or preoperative radiation therapy were excluded, and 69 patients were included. Informed consent was obtained from all patients for the use of tissue samples and clinical data, and this study was approved by the Kobe University Institutional Review Board (B210103). Surgically resected specimens were fixed in 10% formalin and embedded in paraffin. Histologic and clinicopathologic parameters were categorized according to the Japanese Classification of Esophageal Cancer, 10th Edition,[18,19] and TNM classification was determined according to the Union for International Cancer Control TNM Classification of Malignant Tumors, 7th Edition.[20]

Immunohistochemistry

Immunohistochemistry was performed on sections (4 μm thick) of paraffin-embedded tissue using the Leica BOND-MAX automated system and the BOND Polymer Refine Detection Kit (Leica Biosystems). Rabbit antibody against periostin (1:500; number ab14041; Abcam) was used as the primary antibody. Periostin expression was assessed as the percentage of periostin-positive area within the overall cancer stroma area at ×40 magnification. Staining intensity was not included in the decision. The percentage of periostin-positive areas was scored in five grades: 0 ($\leq$1%); 1 (>1% and $\leq$5%); 2 (>5% and $\leq$30%); 3 (>30% and $\leq$50%); and 4 (>50%). Scores of 0, 1, and 2 were defined as low expression, and scores of 3 and 4 were considered high expression (>30%). Immunostaining was evaluated by two pathologists (Y.I.K. and H.Y.) and one surgeon (S.M.) who were blinded to the patients' clinicopathologic data.

Statistical Analysis

All *in vitro* experiments were performed in triplicate and independently conducted three times. Data are expressed as means ± SEM, and statistical significance was analyzed using two-sided *t*-test and Tukey-Kramer tests when comparing more than two groups. The relationships between clinicopathologic factors and immunohistochemical results were estimated using the χ^2 test. OS, disease-free survival, and cancer-specific survival were evaluated with Kaplan-Meier curves and analyzed using the log-rank test. The significance of parameters in univariate and multivariate analyses was assessed using the Cox proportional hazard regression model. $P < 0.05$ was considered significant. Statistical analyses were performed using SPSS software version 22 (IBM, Chicago, IL).

Results

ESCC Cells Show Enhanced Survival, Growth, and Migration on Direct Co-Culture with MSCs through Phosphorylation of Akt and Erk

A direct co-culture system was established between ESCC cell lines (TE-9, TE-10, and TE-15) and MSCs; these cells were also mono-cultured and used as controls. The co-cultured and mono-cultured cells were separated through magnetic-activated cell sorting after 4 days of incubation (Figure 1A). TE cells in mono-culture were defined as TE mono (TE-9 mono, TE-10 mono, and TE-15 mono), MSCs in mono-culture were defined as MSC mono, TE cells after direct co-culture were defined as TE co (TE-9 co, TE-10 co, and TE-15 co), and MSCs after direct co-culture were defined as CAF-like cells (CAF9, CAF10, and CAF15). RT-PCR showed expression of the mesenchymal marker ACTA2 in CAF9, CAF10, and CAF15 compared with MSC mono. In contrast, no expression of the epithelial markers EPCAM and CDH1 was seen (Figure 1B and Supplemental Figure S1A). In addition, EPCAM and CDH1, but not ACTA2, expression was observed in TE-9, TE-10, and TE-15 cells in mono-culture and direct co-culture. Similar results were observed with Western blot analysis (Figure 1B and Supplemental Figures S1B and S2A), confirming the separation of CAF-like cells and TE cells (TE co) from direct co-culture. Furthermore, qPCR and Western blot analysis confirmed that the CAF marker FAP was highly expressed in CAF9, CAF10, and CAF15 (Figure 1, B and C), indicating that MSCs acquired CAF-like properties after direct co-culture. In addition, IL-6, secreted by CAFs, as well as MT2A and SERPINE1, which were up-regulated in CAFs in a previous study,[10,13,14] were highly expressed in CAF9 and CAF10 after direct co-culture (Supplemental Figure S2B). High IL-6 and MT2A expression levels were observed, but SERPINE1 expression decreased in CAF15 (Supplemental Figure S2B). Next, MTS and Transwell migration assays were performed to examine the effects of direct co-culture on TE cells. Survival, growth, and migration were significantly promoted in TE-9, TE-10, and TE-15 cells after direct co-culture with MSCs compared with their respective mono-cultures (Figure 1, D and E). The expression levels of p-Akt (Ser473), p-Akt (Thr308), and phosphorylated Erk increased in TE co (TE-9 co, TE-10 co, and TE-15 co) and CAF9 and CAF10 (Figure 1F and Supplemental Figure S2C). p-Akt (Ser473) expression increased in CAF15, but p-Akt (Thr308) and phosphorylated Erk were not elevated (Figure 1F and Supplemental Figure S2C). These results suggest that survival, growth, and migration of TE cells after direct co-culture are promoted through activation of the Akt and Erk pathways.

Periostin Secreted by CAF Promotes the Migration and Survival of ESCC Cells

The cDNA microarray analysis was performed to examine gene expression changes in CAF-like cells

after direct co-culture relative to mono-cultured MSCs. In a previous study,[13] cDNA microarray analysis was performed to examine gene expression changes in CAF-like cells after indirect co-culture relative to mono-cultured MSCs. To focus on genes elevated in direct co-culture, rather than indirect co-culture, a Venn diagram (Figure 2A) was prepared by cross-checking the results of the present and previous cDNA microarray analyses. In the Venn diagram, 328 genes with a direct CAF9/MSC ratio of twofold or greater (ie, prominently increased) and 1464 genes with an indirect CAF9/MSC ratio of onefold or greater, but less than 1.5-fold (ie, same or mildly increased) in indirect co-culture were detected, and 79 genes in the region where the two groups overlap were identified (Figure 2A). The 79 genes were sorted in descending order of signal intensity by direct CAF9 produced via direct co-culture, identifying transforming growth factor-β (TGF-β) induced (*TGFBI*), periostin (*POSTN*), inhibin A (*INHBA*), protein kinase C β (*PRKCB*), and others (Figure 2A and Table 1). The authors focused on *POSTN*, the gene with the second highest signal intensity, because its overexpression is reportedly involved in various cancer progression in recent years, and its association with CAFs has been reported. The expression of POSTN mRNA increased significantly in CAF9, CAF10, and CAF15 compared with MSCs (Figure 2B). The concentration of periostin secreted from CAF9, CAF10, and CAF15 increased significantly compared with MSCs (Figure 2C). In contrast, little periostin secretion was observed in TE cells in either mono-culture or direct co-culture (Supplemental Figure S3A). Next, the biological effects of periostin on TE cell survival, growth, and migration were examined. Transwell migration and wound healing assays showed that rhPOSTN significantly promoted the migration of TE-9, TE-10, and TE-15 cells (Figure 2, E and F). MTS assays showed that rhPOSTN slightly promoted the survival of TE-9, TE-10, and TE-15 cells, but no changes in growth were observed (Figure 2D). Then, to examine whether the enhancement of TE cell survival, growth, and migration under direct co-culture was dependent on periostin derived from co-cultured MSCs, *POSTN* was knocked down by siRNA in the co-culture system. CAF9, CAF10, and CAF15 from the direct co-culture system with siRNA targeting *POSTN* showed significantly reduced POSTN mRNA expression and periostin secretion compared with that in the direct co-culture system with negative control siRNA (Figure 3, A and B). Moreover, TE-9 co, TE-10 co, and TE-15 co from the direct co-culture system with siRNA targeting *POSTN* showed reduced survival and migration but no change in growth compared with those from the direct co-culture system with negative control siRNA (Figure 3, C and D).

The Enhancement of ESCC Cell Migration and Survival by Periostin Is Due to the Activation of Akt and Erk Pathways via Integrin β4

In TE-9, TE-10, and TE-15 cells, p-Akt (Ser473), p-Akt (Thr308), and phosphorylated Erk levels increased at 10 or 30 minutes after rhPOSTN addition (Figure 4A and Supplemental Figure S3B). Therefore, it was investigated whether the inhibition of Akt or Erk signaling pathway could suppress the periostin-induced phenotypes. In the Transwell migration assays, treatment with phosphatidylinositol 3-kinase inhibitor (LY294002) or MEK1/2 inhibitor (PD98059) significantly suppressed the rhPOSTN-induced enhancement of migration (Figure 4B). The enhancement of the malignant phenotypes of TE-9, TE-10, and TE-15 cells by rhPOSTN was therefore attributed to activation of the Akt and Erk pathways. Next, periostin acts on the integrin family of receptors; thus, the authors focused on integrin β4, whose involvement in ESCC progression was recently reported.[16] The comparison of integrin β4 (ITGB4) expression in TE-9, TE-10, and TE-15 cells after mono-culture and direct co-culture showed increased expression at the mRNA and protein levels under co-culture conditions (Figure 5, A and B, and Supplemental Figure S4A). *ITGB4* was knocked down in TE-9, TE-10, and TE-15 cells using siRNA targeting *ITGB4* (Figure 5, C–E, and Supplemental Figure S4B), which inhibited rhPOSTN-induced migration (Figure 5F and Supplemental Figure S5B). In the MTS assay, rhPOSTN survival enhancement was canceled by *ITGB4* knockdown, but growth remained unchanged (Supplemental Figure S5A). Phosphorylated Akt and Erk pathways, which were enhanced by rhPOSTN, were reduced by *ITGB4* knockdown in TE-9, TE-10, and TE-15 cells (Figure 5G and Supplemental Figure S4C).

Periostin Contributes to the Enhancement of MSC and Macrophage Migration and the Activation of TAM-Like Macrophage Properties

Next, the effect of periostin on MSCs and macrophages was examined. The expression levels of FAP and α-smooth muscle actin were compared in rhPOSTN-treated and untreated MSCs, but no change was observed (Figure 6, A and B, and Supplemental Figure S6). On the other hand, rhPOSTN enhanced MSC migration (Figure 6C). Meanwhile, to examine the effect of periostin on macrophages, peripheral blood monocyte–derived macrophages were cultured with or without rhPOSTN (Figure 7A). rhPOSTN increased the expression levels of the tumor-associated macrophage (TAM) markers CD163 and CD204, along with the percentage of CD163- and CD204-expressing cells; IL-10 expression increased and IL-12 expression decreased at the mRNA level, showing an M2-like phenotype (Figure 7, B–D, and Supplemental Figure S7). Periostin

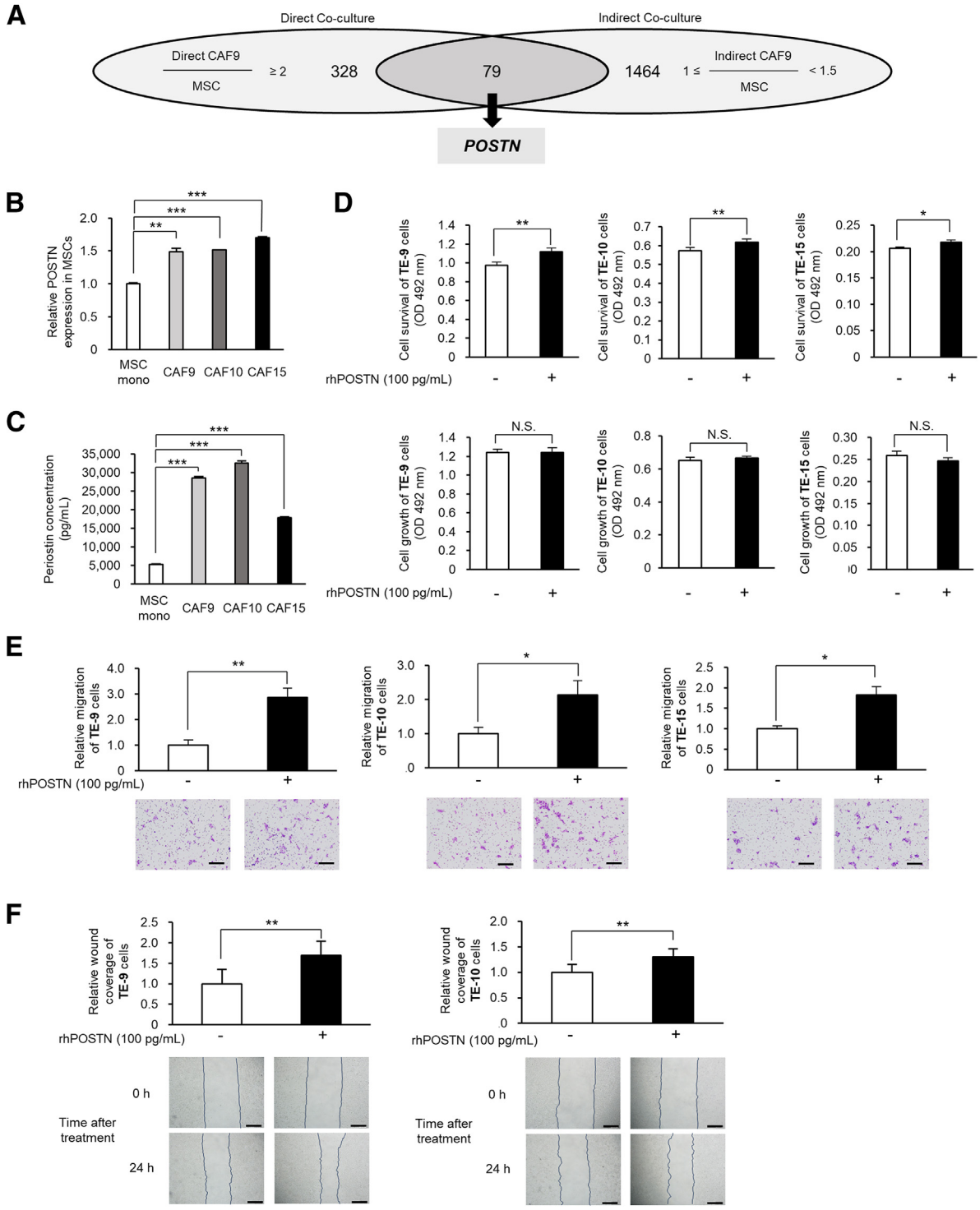

Figure 2 Periostin (POSTN) secreted by cancer-associated fibroblasts (CAFs) promotes migration and survival of esophageal squamous cell carcinoma cells. **A:** Venn diagram of 328 genes with a direct CAF9/mesenchymal stem cell (MSC) ratio of 2-fold or greater in direct co-culture and 1464 genes with an indirect CAF9/MSC ratio of 1-fold to 1.5-fold in indirect co-culture in cDNA microarray analysis. Seventy-nine genes were identified in the region where the two groups overlap in the Venn diagram, and *POSTN* was one of them. **B** and **C:** Expression levels of POSTN and secreted concentrations of periostin in CAF9, CAF10, and CAF15 cells were compared with those in MSCs using real-time quantitative PCR (**B**) and enzyme-linked immunosorbent assay (**C**), respectively. **D:** MTS assays were performed to determine the effect of recombinant human periostin (rhPOSTN; 100 pg/mL) on survival (**top panels**) and growth (**bottom panels**) in TE-9, TE-10, and TE-15 cells. **E:** Transwell migration assays were performed to determine the effect of rhPOSTN (100 pg/mL) on the migration of TE-9, TE-10, and TE-15 cells. Migrating cells were counted in five random fields in each chamber after 48 hours of incubation. Typical images are shown below. **F:** Wound healing assays were performed to determine the effect of rhPOSTN (100 pg/mL) on the horizontal migration of TE-9 and TE-10 cells. The percentage of wound coverage relative to the initial wound was calculated after 24 hours of culture. Typical images are shown below. **Black lines** represent the wound edge of TE-9 and TE-10 cells. Data are presented as means ± SEM (**B**–**F**). $*P < 0.05$, $**P < 0.01$, and $***P < 0.001$. Scale bars = 100 μm (**E** and **F**). N.S., not significant.

Table 1 Up-Regulated Genes in CAF9 Established through Direct Co-Culture, Compared with the Indirect Co-Culture System

Gene accession* (probe ID)	Symbol	Description	Global normalization				Ratio	
			Direct co-culture		Indirect co-culture		Direct co-culture	Indirect co-culture
			CAF9	MSC mono	CAF9	MSC mono	CAF9/MSC	CAF9/MSC
NM_000358.2 (H200012149)	*TGFBI*	Transforming growth factor-β induced	44,297	10,710	14,937	10,762	4.14	1.39
XM_005266232.2 (H300000923)	*POSTN*	Periostin, osteoblast-specific factor	14,427	6350	12,092	10,019	2.27	1.21
NM_000358.2 (AHsV10000051)	*TGFBI*	Transforming growth factor-β induced	14,306	2618	7210	5546	5.47	1.3
NM_002192.2	*INHBA*	Inhibin β A subunit	10,965	3052	2532	2340	3.59	1.08
NG_029003.1	*PRKCB*	Protein kinase C β	10,166	4975	4494	3604	2.04	1.25
XM_011514564.1	*HLA-F*	Major histocompatibility complex, class I, F	9994	4272	6375	4757	2.34	1.34
XM_005266232.2 (AHsV10002160)	*POSTN*	Periostin, osteoblast-specific factor	9242	3992	8996	7683	2.32	1.17
NM_139266.2	*STAT1*	Signal transducer and activator of transcription 1	7035	1134	580	481	6.2	1.2
NM_001278074.1	*COL5A1*	Collagen type V α 1 chain	6165	2605	2333	2046	2.37	1.14
XM_005250234.2	*AKR1B1*	Aldo-keto reductase family 1, member B1 (aldose reductase)	6116	2404	1690	1338	2.54	1.26

*According to DNA sequences at the National Center for Biotechnology Information (*https://www.ncbi.nlm.nih.gov*, last accessed December 1, 2023).
CAF, cancer-associated fibroblast; ID, identifier; MSC mono, mesenchymal stem cell in mono-culture.

also promoted macrophage migration as well as MSC migration (Figure 7E).

Periostin Expression Levels in ESCC Tissues Are Associated with Clinicopathologic Factors and Poor Prognosis in Patients with ESCC

Whether the intensity of periostin expression in ESCC tissues correlated with the clinicopathologic factors of patients with ESCC and their prognosis was investigated next. In 69 patients with ESCC, immunohistochemistry for periostin was performed to evaluate its expression levels in the stroma of invasion area in the low- and high-expression groups (Figure 8A). High periostin expression was associated with depth of tumor invasion ($P < 0.001$), presence of lymphatic vessel invasion ($P = 0.001$), presence of blood vessel invasion ($P < 0.001$), higher pathologic stage ($P = 0.025$), expressions of α-smooth muscle actin ($P < 0.001$) and FAP ($P < 0.001$), and infiltrating numbers of CD68-positive ($P = 0.012$), CD163-positive ($P = 0.001$), and CD204-positive ($P < 0.001$) macrophages (Table 2[18–21]). Sixty-eight patients with ESCC (one dropped out postoperatively) were subsequently followed up to evaluate postoperative outcomes. Kaplan–Meier analysis showed that OS, disease-free survival, and cancer-specific survival were significantly shorter in patients with high periostin expression in the cancer stroma than in those with low expression ($P = 0.004$, $P = 0.003$, and $P = 0.021$, respectively) (Figure 8B). However, multivariate analysis showed that high expression of periostin was not an independent prognostic factor for OS (Table 3[18–21]).

Discussion

Direct co-culture systems can easily reproduce *in vivo* complexity by allowing direct signaling among heterologous cells through cell adhesion molecules, gap junctions, and nanotubes, resulting in intimate interactions.[22–24] Compared with the conventional indirect co-culture system, direct co-culture is more similar to the actual TME, and it can detect promoters or suppressors that cannot be found via the indirect co-culture system.[24,25] Although it requires a few complicated techniques, it is highly reproducible in experiments.[26] In the co-culture of pancreatic ductal adenocarcinoma cells with MSCs, the indirect co-culture system induced only inflammatory CAFs, whereas the direct co-culture system induced myofibroblast-like CAFs, as well as inflammatory CAFs.[27] In laryngeal cancer, fibroblasts directly co-cultured with tumor cells stimulated matrix metalloproteinase-2 production, which promoted invasion and metastasis.[28] Separation of ESCC cells and TAMs using magnetic-activated cell sorting targeting EpCAM after their direct co-culture has been reported previously.[15] Separation of CAFs through negative selection using magnetic-activated cell sorting targeting EpCAM after direct co-culture of gastric cancer cells and CAFs has also

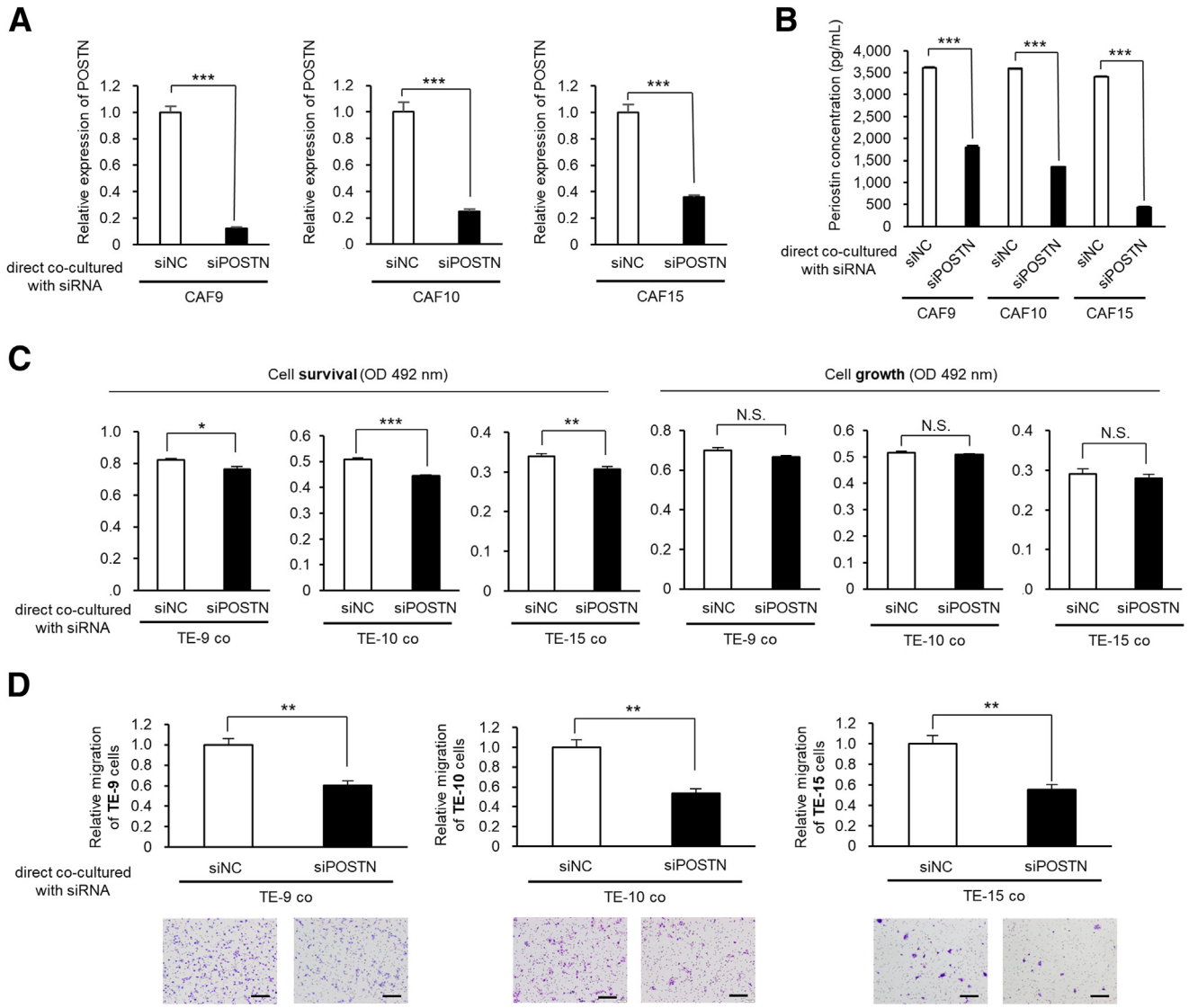

Figure 3 Knockdown of *POSTN* in direct co-culture system attenuates the survival and migration of esophageal squamous cell carcinoma cells enhanced by direct co-culture with mesenchymal stem cells (MSCs). **A** and **B:** Cancer-associated fibroblast (CAF) 9, CAF10, and CAF15 cells were separated from direct co-culture system transfected with siRNA targeting *POSTN* (siPOSTN; 20 nmol/L) and negative control siRNA (siNC; 20 nmol/L). **A** and **B:** *POSTN* knockdown in CAF-like cells was confirmed using real-time quantitative PCR (qPCR; **A**) and enzyme-linked immunosorbent assay (**B**). Glyceraldehyde-3-phosphate dehydrogenase (GAPDH) was used as a control in qPCR. **C:** MTS assays were performed to confirm the effect of *POSTN* knockdown on the enhanced survival (**left panels**) and growth (**right panels**) of TE-9, TE-10, and TE-15 cells by direct co-culture with MSCs. **D:** Transwell migration assays were performed to determine the effect of *POSTN* knockdown on the enhanced migration of TE-9, TE-10, and TE-15 cells by direct co-culture with MSCs. Migrating cells were counted in five random fields in each chamber after 48 hours of incubation. Typical images are shown below. Data are presented as means ± SEM (**A**–**D**). $*P < 0.05$, $**P < 0.01$, and $***P < 0.001$. Scale bars = 100 μm (**D**). N.S., not significant.

been reported.[29] In the present study, ESCC cells and MSCs were separated using magnetic-activated cell sorting targeting EpCAM from their direct co-culture. MSCs after direct co-culture showed high expression of FAP, a CAF marker, and high expression of IL-6 and MT2A, which are highly expressed in CAF,[10,14] indicating that CAF-like cells were successfully generated. SERPINE1, which is highly expressed in CAFs after indirect co-culture,[13] was not highly expressed in direct co-culture with one ESCC cell line (TE-15), which was attributed to differences in the system used to prepare the CAF-like cells. The direct co-culture system enhanced the malignant phenotypes, such as survival, growth, and migration of ESCC cell lines, similar to the indirect co-culture.

TGFBI and *POSTN* were the top two significantly up-regulated genes under direct co-culture while being unchanged or mildly up-regulated under indirect co-culture. Both encode extracellular matrix proteins with a 48% structural similarity, but TGFBI has Arg-Gly-Asp (RGD) sequences and is involved in cell adhesion, unlike

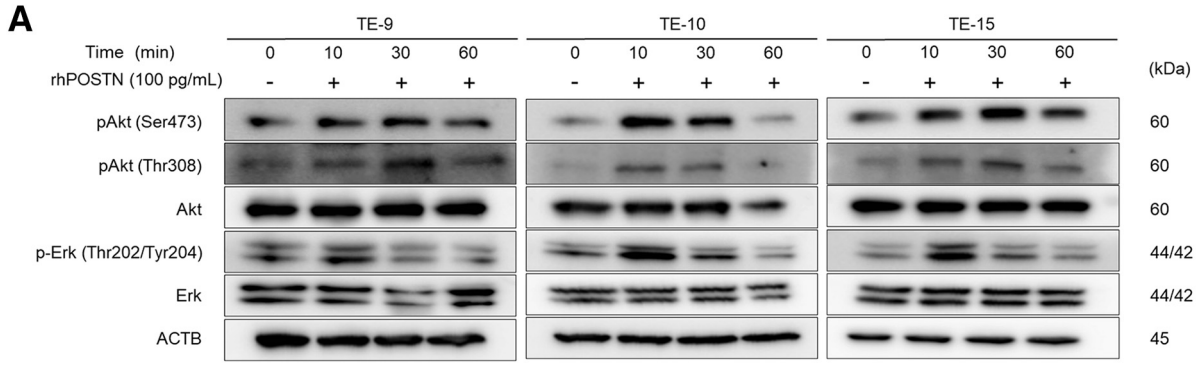

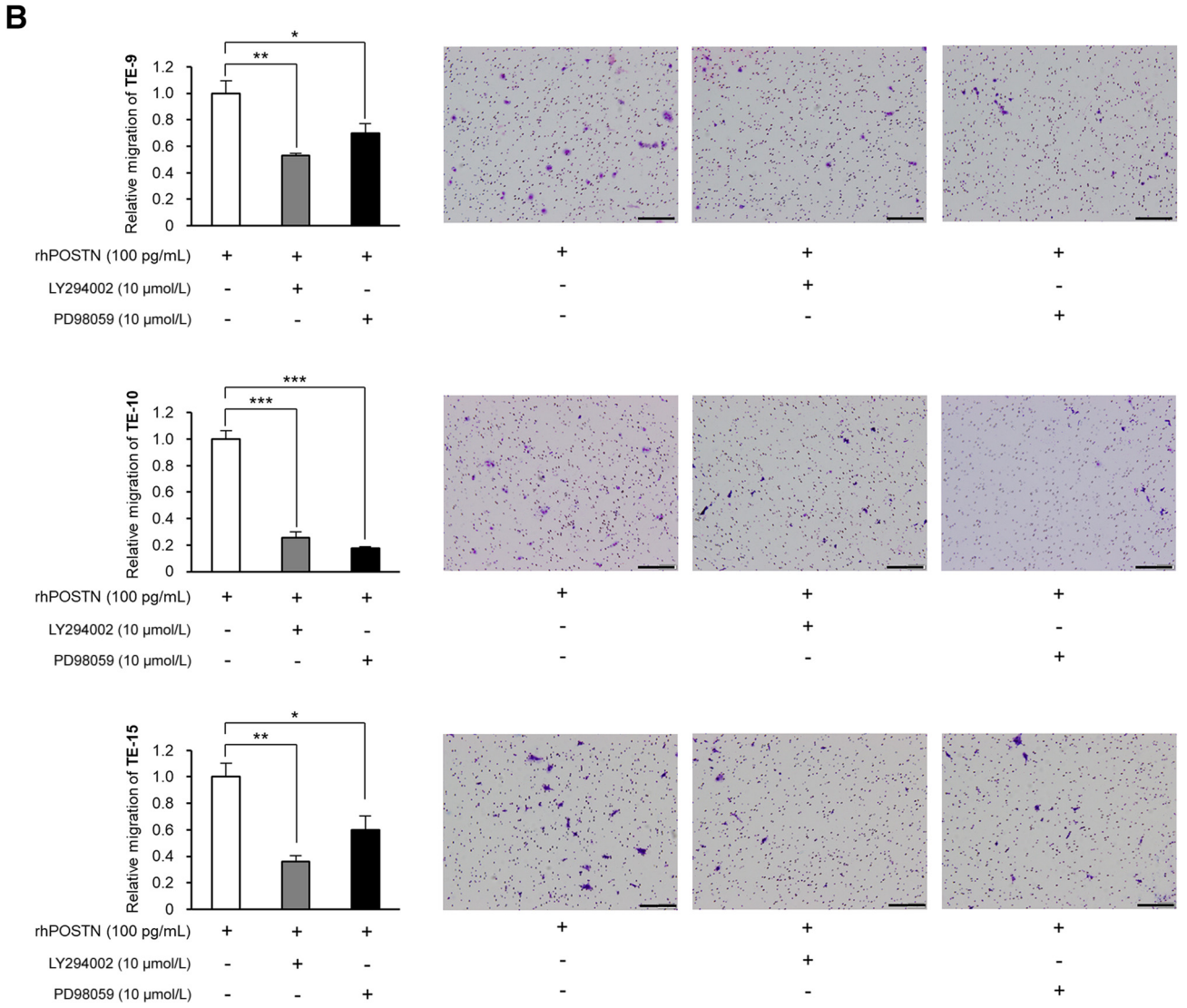

Figure 4 Periostin promotes migration through Akt and extracellular signal-regulated kinase (Erk) signaling pathways in esophageal squamous cell carcinoma cells. **A:** Time-dependent changes in Akt, phosphorylated Akt (p-Akt; Ser473), p-Akt (Thr308), Erk, and phosphorylated Erk (p-Erk; Thr202/Tyr204) levels in TE-9, TE-10, and TE-15 cells treated with recombinant human periostin (rhPOSTN) were confirmed via Western blot analysis using beta actin (ACTB) as a control. **B:** Transwell migration assays were performed to determine changes in the migration of TE-9, TE-10, and TE-15 cells following rhPOSTN (100 pg/mL) treatment with phosphatidylinositol 3-kinase (PI3K) inhibitor (LY294002; 10 μmol/L) or MEK1/2 inhibitor (PD98059; 10 μmol/L). Migrating cells were counted in five random fields in each chamber after 48 hours of incubation. Typical images are shown to the right. Data are presented as means ± SEM (**B**). $^{*}P < 0.05$, $^{**}P < 0.01$, and $^{***}P < 0.001$. Scale bars = 100 μm (**B**).

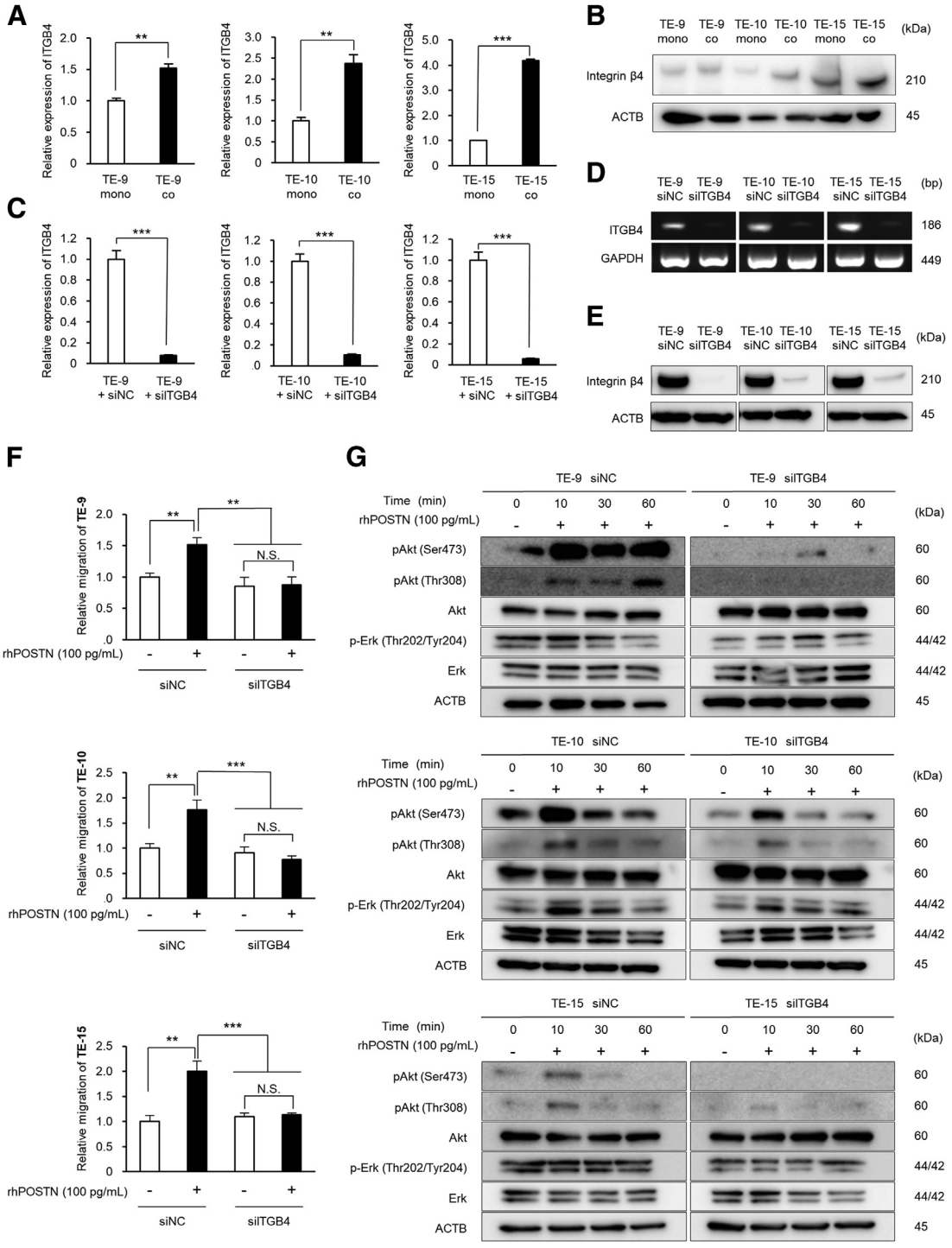

Figure 5 The enhancement of esophageal squamous cell carcinoma cell migration by periostin is mediated via integrin β4. **A** and **B:** Integrin subunit beta 4 (ITGB4) and integrin β4 expression levels in TE cells after direct co-culture were compared with those after mono-culture using real-time quantitative PCR (qPCR; **A**) and Western blot analysis (**B**). Beta actin (ACTB) was used as a control in the Western blot analysis. **C**—**E:** TE-9, TE-10, and TE-15 cells were transfected with siRNA targeting *ITGB4* (siITGB4; 20 nmol/L) and negative control siRNA (siNC; 20 nmol/L). *ITGB4* knockdown was confirmed using qPCR (**C**), RT-PCR (**D**), and Western blot analysis (**E**). Glyceraldehyde-3-phosphate dehydrogenase (GAPDH) and ACTB were used as a control in RT-PCR and Western blot analysis, respectively. **F:** Transwell migration assays were performed to confirm the effect of *ITGB4* knockdown on the enhanced migration of TE-9, TE-10, and TE-15 cells by adding recombinant human periostin (rhPOSTN; 100 pg/mL). Migrating cells were counted in five random fields in each chamber after 48 hours of incubation. **G:** TE-9, TE-10, and TE-15 cells transfected with siNC and siITGB4 were treated with rhPOSTN (100 pg/mL), and time-dependent changes in Akt, phosphorylated Akt (p-Akt; Ser473), p-Akt (Thr308), extracellular signal-regulated kinase (Erk), and phosphorylated Erk (p-Erk; Thr202/Tyr204) levels in each cell were then determined using Western blot analysis. ACTB was used as a control. Data are presented as means ± SEM (**A**, **C**, and **F**). $^{**}P < 0.01$, $^{***}P < 0.001$. N.S., not significant.

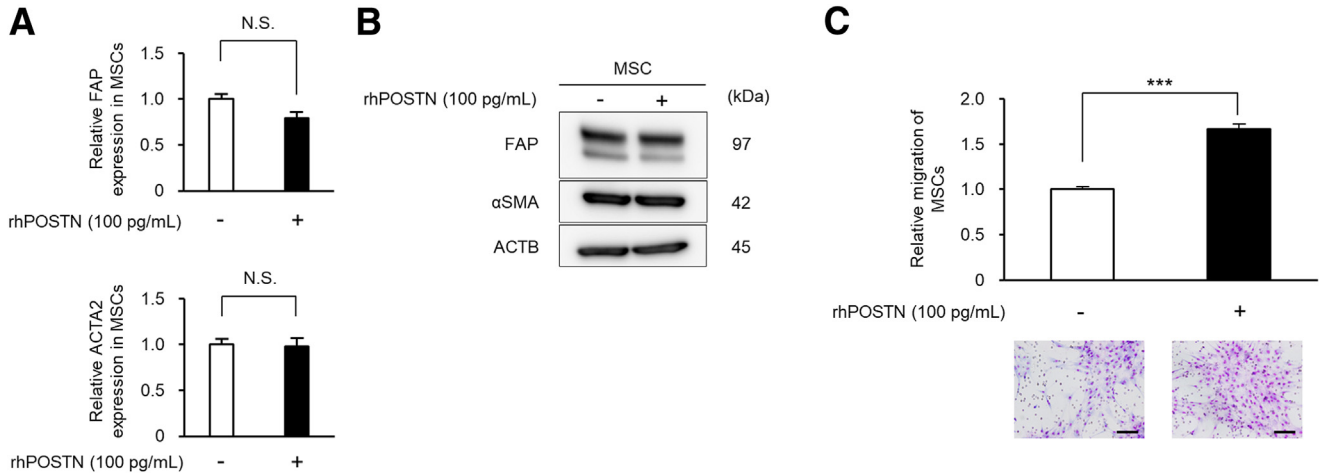

Figure 6 Periostin is not related to acquired cancer-associated fibroblast (CAF)—like properties in mesenchymal stem cells (MSCs), but it contributes to enhancing their migration. **A:** Fibroblast activation protein (FAP) and actin alpha 2 (ACTA2) expression levels in recombinant human periostin (rhPOSTN)—treated and untreated MSCs were compared via real-time quantitative PCR. **B:** FAP and α-smooth muscle actin (α-SMA) expression levels in rhPOSTN-treated and untreated MSCs were compared via Western blot analysis. Beta actin (ACTB) was used as a control. **C:** Transwell migration assays were performed to confirm the migration of rhPOSTN-treated and untreated MSCs. Migrating cells were counted in five random fields in each chamber after 48 hours of incubation. Typical images are shown below. $***P < 0.001$. Scale bars = 100 μm (**C**). N.S., not significant.

periostin.[30] In addition, TGFBI expression is regulated by TGF-β signaling, whereas periostin expression is not.[30–32] However, Qin et al[33] reported that TGF-β3 mediates induction of periostin facilitates head and neck cancer growth and is associated with metastasis. Yue et al[34] recently reported that periostin induced by TGF-β1 promotes the migration and invasion of ovarian cancer, suggesting that TGF-β1 and TGF-β3 are involved in periostin regulation. However, there is no report yet indicating that TGFBI regulates periostin expression. The role of TGFBI in cancer is controversial, with reports of TGFBI as a tumor-promoting factor in ESCC and gastric cancer.[35,36] In contrast, some reports also show TGFBI as a tumor suppressor in non—small-cell lung cancer[37] and breast cancer[38] and as a chemotherapy sensitivity promoter in lung cancer.[39,40] On the other hand, periostin overexpression has been reported in a variety of solid epithelial tumors, and there are many reports that its interaction with integrin surface receptors regulates intracellular signaling pathways promoting cancer progression.[41] In contrast, periostin is a metastasis suppressor only in bladder cancer,[42] and mutational analysis has shown that the C-terminal region of periostin is responsible for this effect.[43] Therefore, periostin, which is more frequently reported as a tumor-promoting factor, was selected as more likely to be more clinically significant and focused on in this study.

Periostin is a 90-kDa protein primarily secreted by CAFs in the TME.[41] Many positive correlations between periostin overexpression and malignant phenotypes have been reported in various cancers, including non—small-cell lung cancer,[44,45] breast cancer,[46,47] colorectal cancer,[48,49] pancreatic cancer,[50,51] head and neck cancer,[33,52] and oral cancer.[53] However, only two groups reported that periostin promoted the malignant phenotype of ESCC.[54,55]

Periostin binds to integrins αvβ3, αvβ5, and α6β4 on the target cell surface and is known to activate multiple signaling pathways.[41] Activation of the Erk/NF-κB signaling pathway via αvβ3 in breast cancer increases *IL6* and *IL8* transcription and promoted cancer stem cell maintenance.[56] Furthermore, Akt signaling pathway activation via αvβ3 in colorectal cancer inhibits the apoptosis of tumor cells and endothelial cells and promotes angiogenesis.[49] Yan and Shao[57] also reported that periostin promotes epithelial-mesenchymal transition by binding to integrin αvβ5 in concert with epidermal growth factor receptor signaling in experiments using epithelial-derived 293T cells with forced periostin expression. Integrin β4 is a subunit that forms a heterodimer with only integrin α6.[58] Some reports show that periostin affects cancer malignant phenotypes via integrin α6β4, activating the phosphatidylinositol 3-kinase inhibitor/Akt pathway to promote epithelial-mesenchymal transition and migration in colorectal cancer,[59] as well as tumor invasion and resistance to hypoxia-induced apoptosis in pancreatic ductal adenocarcinoma.[50] In ESCC, Ishibashi et al[60] reported that periostin activates the Erk pathway via αvβ3 or αvβ5 and promoted proliferation and migration. However, to the best of our knowledge, no report has shown a periostin-integrin α6β4 relationship in ESCC. Integrin α6β4 heterodimers promote ESCC growth and invasion,[61] and integrin β4 mediated effects on YKL-40/osteopontin in early ESCC.[16] Thus, integrin β4 expression in ESCC cells may be significant. Herein, periostin enhanced the migration and survival of ESCC cells via the Akt and Erk pathways, and integrin β4 knockdown canceled these enhancements, indicating that periostin produced by CAFs promotes migration and survival via integrin β4 on the ESCC cell surface.

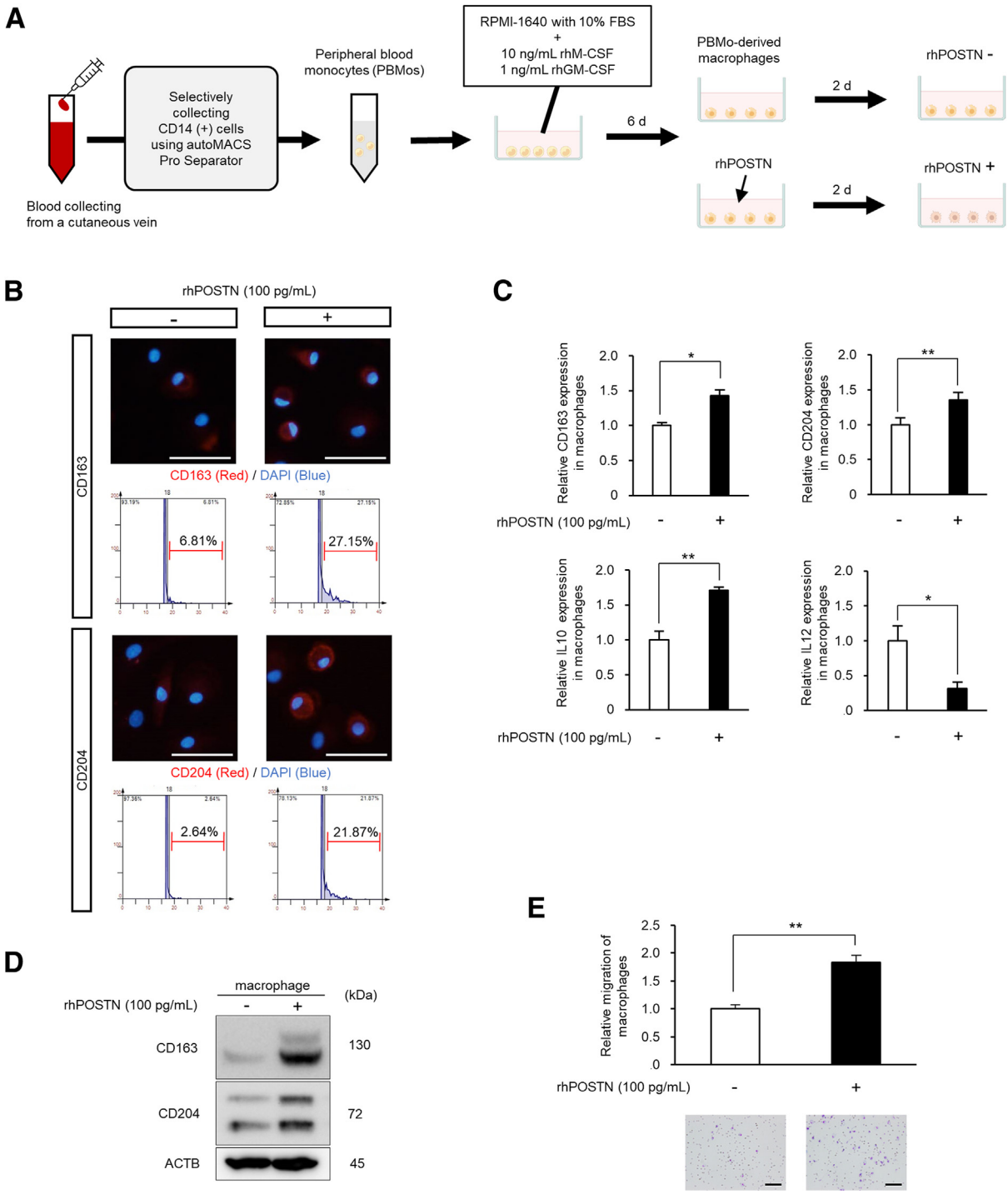

Figure 7 Periostin contributes to the acquisition of tumor-associated macrophage (TAM)—like properties in macrophages and enhances their migration. **A:** $CD14^{+}$ peripheral blood monocytes (PBMos) were selectively collected from human peripheral blood using magnetic-activated cell sorting (MACS) and treated with recombinant human macrophage colony-stimulating factor (rhM-CSF; 10 ng/mL) and recombinant human granulocyte-macrophage colony-stimulating factor (rhGM-CSF; 1 ng/mL) for 6 days to establish PBMo-derived macrophages. Then, untreated PBMo-derived macrophages and recombinant human periostin (rhPOSTN)—treated PBMo-derived macrophages were cultured for 2 days. **B:** Immunofluorescence of CD163 (red) and CD204 (red) in macrophages treated with or without rhPOSTN (100 pg/mL) for 48 hours. The nuclei were stained with DAPI (blue). The percentage of CD163- or CD204-positive cells in the total number of DAPI-positive macrophages was measured and showed as histograms below. The *x* and *y* axes show the mean intensity of CD163 and CD204 expressions and the number of cells for each sample, respectively. **C:** The expression levels of CD163, CD204, IL-10, and IL-12 in rhPOSTN-treated and untreated macrophages were analyzed using real-time quantitative PCR. **D:** CD163 and CD204 expression levels in rhPOSTN-treated and untreated macrophages were analyzed via Western blot analysis. Beta actin (ACTB) was used as a control. **E:** Transwell migration assays were performed to confirm the migration of rhPOSTN-treated and untreated macrophages. Migrating cells were counted in five random fields in each chamber after 48 hours of incubation. Typical images are shown below. $^{*}P < 0.05$, $^{**}P < 0.01$. Scale bars: 50 μm (**B**); 100 μm (**E**).

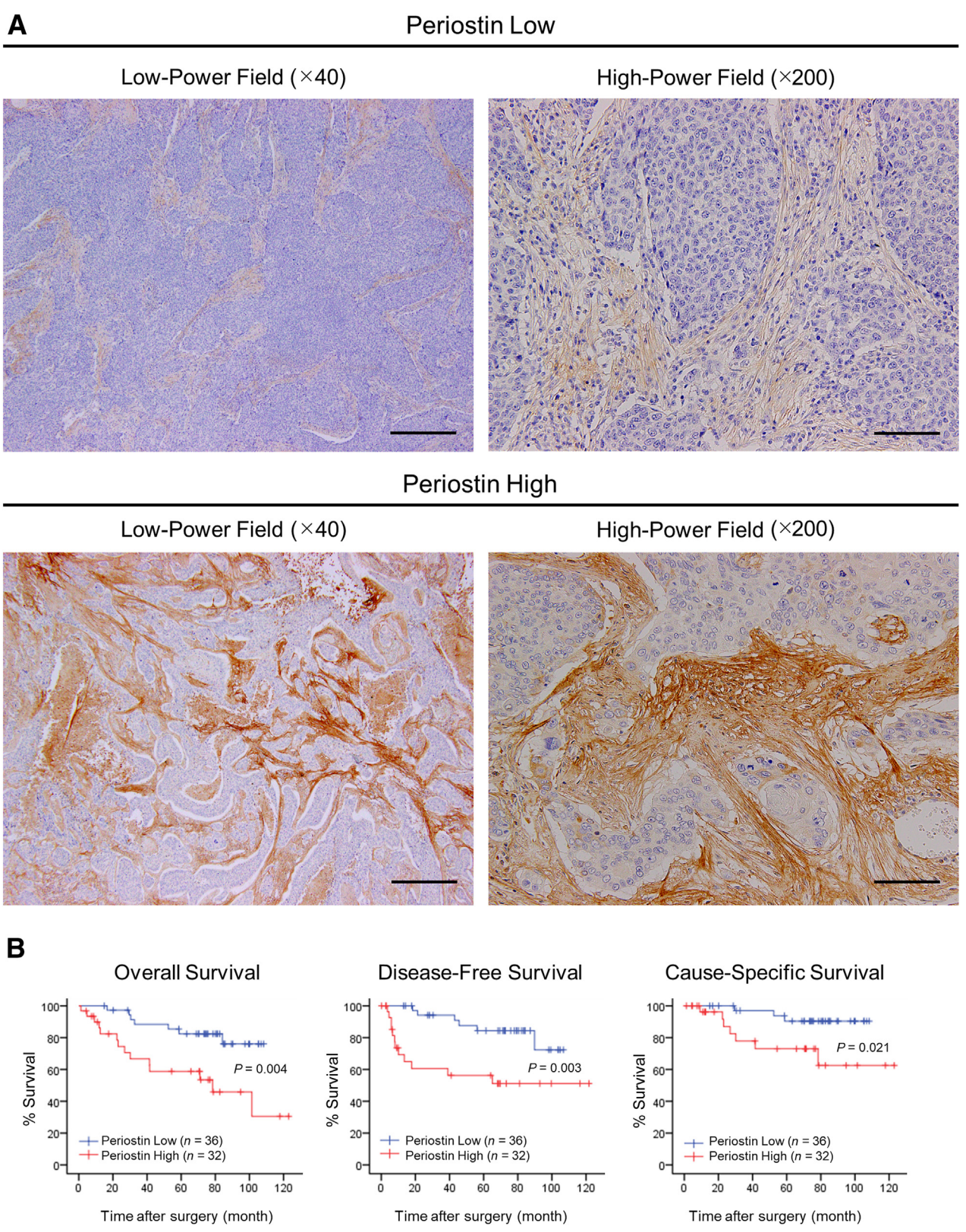

Figure 8 Periostin expression in esophageal squamous cell carcinoma (ESCC) tissue correlates with poor prognosis in patients with ESCC. **A:** Periostin expression in 69 human ESCC tissues was evaluated immunohistochemically. On the basis of the intensity of stromal periostin staining in the invasive areas, samples were classified into two groups: the low periostin group and the high periostin group. Representative low- and high-magnification images of ESCC tissue are shown. **B:** Kaplan—Meier analysis of overall survival (OS), disease-free survival (DFS), and cancer-specific survival (CSS) in 68 patients with ESCC with low and high periostin expression; *P* values were determined using the log-rank test. $n = 37$ (**A**, low periostin expression); $n = 32$ (**A** and **B**, high periostin expression); $n = 36$ (**B**, low periostin expression). Scale bars: 400 μm (**A**, **left panels**); 100 μm (**A**, **right panels**).

Table 2 Relationship between POSTN Expression Levels and Clinicopathologic Factors

Variable	*N*	Expression of POSTN		*P* value
		Low ($n = 37$)	High ($n = 32$)	
Age, years				
<65	32	16	16	0.575
≥65	37	21	16	
Sex				
Male	14	7	7	0.761
Female	55	30	25	
Histologic grade[18,19]				
HGIEN + WDSCC	15	10	5	0.252
MDSCC + PDSCC	54	27	27	
Depth of tumor invasion[18,19]				
T1	48	34	14	<0.001***
T2 + T3	21	3	18	
Lymphatic vessel invasion[18,19]				
Negative	37	27	10	0.001**
Positive	32	10	22	
Blood vessel invasion[18,19]				
Negative	43	29	14	<0.001***
Positive	26	8	18	
Lymph node metastasis[18,19]				
Negative	43	27	16	0.050
Positive	26	10	16	
Stage[20]				
0 + I	38	25	13	0.025*
II + III + IV	31	12	19	
Expression of α-SMA[10]				
Low	36	31	5	<0.001***
High	33	6	27	
Expression of FAP[10]				
Low	39	30	9	<0.001***
High	30	7	23	
Expression of CD68[21]				
Low	35	24	11	0.012*
High	34	13	21	
Expression of CD163[21]				
Low	34	25	9	0.001**
High	35	12	23	
Expression of CD204[21]				
Low	34	27	7	<0.001***
High	35	10	25	

Data were analyzed using a χ^2-test. $P < 0.05$ was considered statistically significant: $^*P < 0.05$, $^{**}P < 0.01$, and $^{***}P < 0.001$.

Reference 10: classified into low and high groups based on the immunoreactivity observed in the invasive front of the tumor. A cutoff value of 30% was established for categorization (high: >30%; low: ≤30%). References 18 and 19: refer to the 10th edition of the Japanese Classification of Esophageal Cancer. Reference 20: refers to the 7th edition of the TNM classification by the Union for International Cancer Control. Reference 21: patients were stratified into low and high groups based on the median number of infiltrating CD68-positive, CD163-positive, or CD204-positive macrophages in the cancer nests and stroma.

FAP, fibroblast activation protein; HGIEN, high-grade intraepithelial neoplasia; MDSCC, moderately differentiated squamous cell carcinoma; PDSCC, poorly differentiated squamous cell carcinoma; POSTN, periostin; α-SMA, α-smooth muscle actin; T1, tumor invades the mucosa and submucosa; T2, tumor invades the muscularis propria; T3, tumor invades the adventitia; WDSCC, well-differentiated squamous cell carcinoma.

Periostin is associated not only with cancer cells, but also with CAFs and TAMs in the TME. Periostin works on tumor cells to secrete TGF-β1 and TGF-β2, causing fibroblasts and human adipose-derived stromal cells to induce CAFs.[34,62] In ovarian cancer, TGF-β1 secreted by periostin-mediated stimulation promotes the migration of fetal lung-derived fibroblasts with acquired CAF-like properties.[34] However, no reports have shown that periostin directly affects MSCs, fibroblasts, or adipocytes, which represent the origin of CAFs, to induce CAFs. In the current study, periostin also promoted MSC migration without acquiring CAF-like properties. In addition, periostin is known to induce macrophage differentiation to TAMs in the TME of glioblastoma and ovarian cancer.[62,63] Periostin also induces

Table 3 Relationship between Clinicopathologic Parameters of Esophageal Squamous Cell Carcinoma and Overall Survival

		Univariate analysis				Multivariate analysis		
Variable	*N*	Medium survival time, months	HR	95% CI	*P* value	HR	95% CI	*P* value
Age, years								
<65	32	97.185	1.671	0.683—4.092	0.256			
≥65	36	73.362						
Sex								
Male	14	103.338	1.999	0.585—6.834	0.260			
Female	54	84.010						
Histologic grade[18,19]								
HGIEN + WDSCC	15	72.052	0.935	0.339—2.582	0.897			
MDSCC + PDSCC	53	90.568						
Depth of tumor invasion[18,19]								
T1	48	98.401	3.233	1.323—7.901	0.007**	1.231	0.375—4.048	0.732
T2 + T3	20	56.719						
Lymphatic vessel invasion[18,19]								
Negative	37	101.765	3.050	1.248—7.458	0.010*	1.712	0.506—5.799	0.387
Positive	31	68.419						
Blood vessel invasion[18,19]								
Negative	43	101.051	3.019	1.247—7.310	0.010*	1.814	0.674—4.882	0.238
Positive	25	60.795						
Lymph node metastasis[18,19]								
Negative	43	94.552	1.544	0.646—3.686	0.325			
Positive	25	75.920						
Stage[20]								
0 + I	38	96.812	1.858	0.782—4.416	0.154			
II + III + IV	30	75.083						
Expression of POSTN								
Low	37	94.294	3.554	1.427—8.849	0.004**	2.619	0.950—7.220	0.063
High	31	71.604						
Expression of α-SMA[10]								
Low	36	98.936	2.082	0.865—5.009	0.095			
High	32	72.811						
Expression of FAP[10]								
Low	39	106.094	4.033	1.615—10.072	0.001**			
High	29	64.522						
Expression of CD68[21]								
Low	35	99.796	1.973	0.802—4.681	0.135			
High	33	78.190						
Expression of CD163[21]								
Low	34	97.554	2.252	0.908—5.585	0.072			
High	34	79.995						
Expression of CD204[21]								
Low	34	99.263	2.204	0.836—4.900	0.111			
High	34	74.826						

Overall survival was estimated using the Kaplan—Meier method and compared using the log-rank test. $P < 0.05$ was considered statistically significant: $^{*}P < 0.05$, $^{**}P < 0.01$.

Reference 10: classified into low and high groups based on the immunoreactivity observed in the invasive front of the tumor. A cutoff value of 30% was established for categorization (high: >30%; low: ≤30%). References 18 and 19: refer to the 10th edition of the Japanese Classification of Esophageal Cancer. Reference 20: refers to the 7th edition of the TNM classification by the Union for International Cancer Control. Reference 21: patients were stratified into low and high groups based on the median number of infiltrating CD68-positive, CD163-positive, or CD204-positive macrophages in the cancer nests and stroma.

FAP, fibroblast activation protein; HGIEN, high-grade intraepithelial neoplasia; HR, hazard ratio; MDSCC, moderately differentiated squamous cell carcinoma; PDSCC, poorly differentiated squamous cell carcinoma; POSTN, periostin; α-SMA, α-smooth muscle actin; T1, tumor invades the mucosa and submucosa; T2, tumor invades the muscularis propria; T3, tumor invades the adventitia; WDSCC, well-differentiated squamous cell carcinoma.

macrophage proliferation during the repair process after acute kidney injury and promotes M2 macrophage migration in pulmonary hypertension.[64,65] Periostin-affected macrophages exhibit high IL-10 expression and low IL-12 expression, which indicates M2-like macrophage polarization, and high CD163 and CD204 expression, which indicates acquisition of TAM-like properties, and newly showed enhanced macrophage migration.

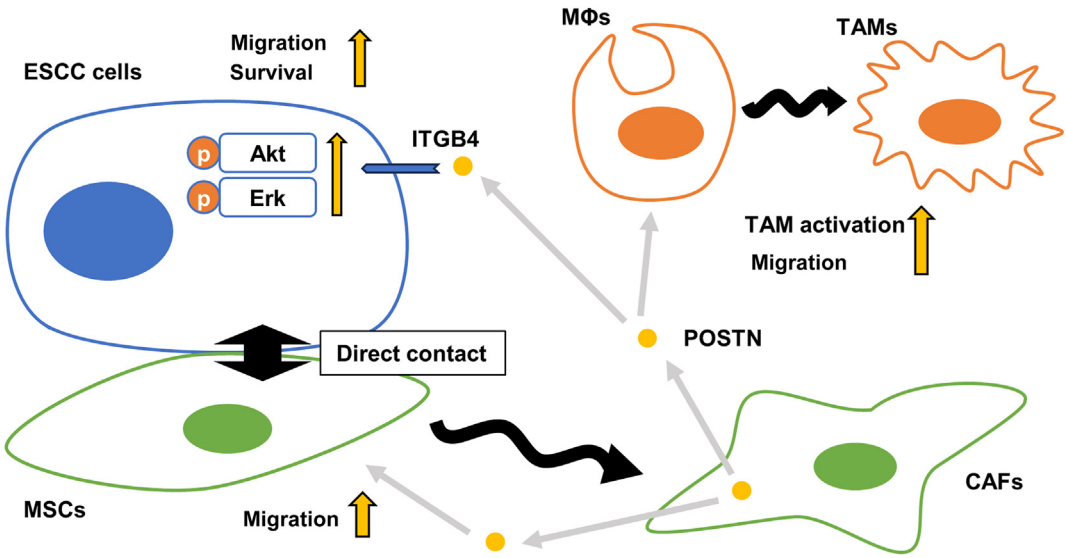

Figure 9 Schematic diagram of roles of periostin (POSTN) in the esophageal squamous cell carcinoma (ESCC) microenvironment. Direct contact with ESCC cells leads mesenchymal stem cells (MSCs) to become cancer-associated fibroblast (CAF)–like cells, which secrete periostin and activate the Akt and extracellular signal-regulated kinase (Erk) pathways via integrin subunit beta 4 (ITGB4) in ESCC cells, promoting their migration. Periostin also promotes MSC and macrophage migration and contributes to the activation of tumor-associated macrophage (TAM)–like macrophage properties. MΦ, macrophage.

As shown in Figure 9, the current results indicated that CAF-like cells generated through direct co-culture with ESCC cells secreted periostin to promote migration and survival via integrin β4 expressed in ESCC cells. This study reports, for the first time, that periostin promotes the malignant phenotype of ESCC cells via integrin β4, promotes the migration of MSCs and macrophages, and induces TAM activation.

High periostin expression in human ESCC tissues was correlated with the depth of tumor invasion, vascular invasion, lymphatic invasion, and advanced pathologic stage, supporting the effect of periostin on ESCC cell migration *in vitro*. Wang et al[55] reported that high periostin expression was correlated with lymph node metastasis, tumor differentiation, venous invasion, and TNM stage, consistent with the current results. For the first time, this study showed that high periostin expression correlated with the α-smooth muscle actin and FAP expressions, suggesting that periostin may be a CAF marker. CD68, a pan-macrophage marker, and CD163 and CD204, TAM markers, were positively correlated with high periostin expression, supporting the *in vitro* results promoting macrophage migration and the acquisition of TAM-like properties. Furthermore, high periostin expression in the cancer stroma correlated with poor OS, disease-free survival, and cancer-specific survival in patients with ESCC. This result is consistent with the results of previously published reports.[54,55,66] Multivariate analysis showed that periostin was not an independent prognostic factor for OS (Table 3), in disagreement with known reports.[54,55] However, approximately two-thirds of cases in those two reports exhibited deeper tumors than T2; in one group,[54] some patients had preoperative treatment, such as neoadjuvant chemotherapy, so its effect cannot be ruled out. In the present study, approximately 70% of the patients exhibited T1 tumor depth, and tissue specimens without neoadjuvant chemotherapy or other treatments were used in all cases. As more samples and clinical data are tracked further, periostin has the potential to be a prognostic factor for OS.

This study has several limitations. First, the sample size for clinical analysis was small. Second, it did not examine the receptors for periostin in macrophages and CAFs. Finally, *in vivo* studies were not included to validate the present results. However, *in vivo* experiments have shown that anti-periostin neutralizing antibodies inhibit proliferation and metastasis in ovarian and breast cancer,[67,68] as well as tumor growth and angiogenesis in melanoma.[69] The inhibitory effect of periostin on ESCC progression needs to be studied *in vivo* using animal models in the future.

In conclusion, the present study established a direct co-culture system between ESCC cells and MSCs, which promoted the malignant phenotype of ESCC cells. Periostin secreted from CAFs mainly promoted survival and migration of ESCC cells, MSC and macrophage migration, and TAM activation, contributing to the development of the TME. High periostin expression in the cancer stroma was positively correlated with progression of clinicopathologic factors and poor survival rates in patients with ESCC. Periostin is expected to be a novel therapeutic target for ESCC progression.

Acknowledgments

We thank Yumi Hashimoto, Nobuo Kubo, and Miki Yamazaki for excellent technical support.

Disclosure Statement

None declared.

Supplemental Data

Supplemental material for this article can be found at *http://doi.org/10.1016/j.ajpath.2023.12.010*.

References

1. Arnold M, Abnet CC, Neale RE, Vignat J, Giovannucci EL, McGlynn KA, Bray F: Global burden of 5 major types of gastrointestinal cancer. Gastroenterology 2020, 159:335–349.e15
2. Short MW, Burgers KG, Fry VT: Esophageal cancer. Am Fam Physician 2017, 95:22–28
3. Abnet CC, Arnold M, Wei WQ: Epidemiology of esophageal squamous cell carcinoma. Gastroenterology 2018, 154:360–373
4. Qiu L, Yue J, Ding L, Yin Z, Zhang K, Zhang H: Cancer-associated fibroblasts: an emerging target against esophageal squamous cell carcinoma. Cancer Lett 2022, 546:215860
5. Pennathur A, Farkas A, Krasinskas AM, Ferson PF, Gooding WE, Gibson MK, Schuchert MJ, Landreneau RJ, Luketich JD: Esophagectomy for T1 esophageal cancer: outcomes in 100 patients and implications for endoscopic therapy. Ann Thorac Surg 2009, 87:1048–1054. discussion 1054-1055
6. Pennathur A, Gibson MK, Jobe BA, Luketich JD: Oesophageal carcinoma. Lancet 2013, 381:400–412
7. Yokozaki H, Koma YI, Shigeoka M, Nishio M: Cancer as a tissue: the significance of cancer-stromal interactions in the development, morphogenesis and progression of human upper digestive tract cancer. Pathol Int 2018, 68:334–352
8. Li H, Fan X, Houghton J: Tumor microenvironment: the role of the tumor stroma in cancer. J Cell Biochem 2007, 101:805–815
9. Sahai E, Astsaturov I, Cukierman E, DeNardo DG, Egeblad M, Evans RM, Fearon D, Greten FR, Hingorani SR, Hunter T, Hynes RO, Jain RK, Janowitz T, Jorgensen C, Kimmelman AC, Kolonin MG, Maki RG, Powers RS, Pure E, Ramirez DC, Scherz-Shouval R, Sherman MH, Stewart S, Tlsty TD, Tuveson DA, Watt FM, Weaver V, Weeraratna AT, Werb Z: A framework for advancing our understanding of cancer-associated fibroblasts. Nat Rev Cancer 2020, 20:174–186
10. Higashino N, Koma YI, Hosono M, Takase N, Okamoto M, Kodaira H, Nishio M, Shigeoka M, Kakeji Y, Yokozaki H: Fibroblast activation protein-positive fibroblasts promote tumor progression through secretion of CCL2 and interleukin-6 in esophageal squamous cell carcinoma. Lab Invest 2019, 99:777–792
11. Yeo SY, Ha SY, Lee KW, Cui Y, Yang ZT, Xuan YH, Kim SH: Twist1 is highly expressed in cancer-associated fibroblasts of esophageal squamous cell carcinoma with a prognostic significance. Oncotarget 2017, 8:65265–65280
12. Galvan JA, Wiprachtiger J, Slotta-Huspenina J, Feith M, Ott K, Kroll D, Seiler CA, Langer R: Immunohistochemical analysis of the expression of cancer-associated fibroblast markers in esophageal cancer with and without neoadjuvant therapy. Virchows Arch 2020, 476:725–734
13. Sakamoto H, Koma YI, Higashino N, Kodama T, Tanigawa K, Shimizu M, Fujikawa M, Nishio M, Shigeoka M, Kakeji Y, Yokozaki H: PAI-1 derived from cancer-associated fibroblasts in esophageal squamous cell carcinoma promotes the invasion of cancer cells and the migration of macrophages. Lab Invest 2021, 101:353–368
14. Shimizu M, Koma YI, Sakamoto H, Tsukamoto S, Kitamura Y, Urakami S, Tanigawa K, Kodama T, Higashino N, Nishio M, Shigeoka M, Kakeji Y, Yokozaki H: Metallothionein 2A expression in cancer-associated fibroblasts and cancer cells promotes esophageal squamous cell carcinoma progression. Cancers (Basel) 2021, 13:4552
15. Tanigawa K, Tsukamoto S, Koma YI, Kitamura Y, Urakami S, Shimizu M, Fujikawa M, Kodama T, Nishio M, Shigeoka M, Kakeji Y, Yokozaki H: S100A8/A9 induced by interaction with macrophages in esophageal squamous cell carcinoma promotes the migration and invasion of cancer cells via Akt and p38 MAPK pathways. Am J Pathol 2022, 192:536–552
16. Urakami S, Koma YI, Tsukamoto S, Azumi Y, Miyako S, Kitamura Y, Kodama T, Nishio M, Shigeoka M, Abe H, Usami Y, Kodama Y, Yokozaki H: Biological and clinical significance of the YKL-40/osteopontin-integrin beta4-p70S6K axis induced by macrophages in early oesophageal squamous cell carcinoma. J Pathol 2023, 261:55–70
17. Nishio M, Urakawa N, Shigeoka M, Takase N, Ichihara Y, Arai N, Koma Y, Yokozaki H: Software-assisted morphometric and phenotype analyses of human peripheral blood monocyte-derived macrophages induced by a microenvironment model of human esophageal squamous cell carcinoma. Pathol Int 2016, 66:83–93
18. Japan Esophageal Society: Japanese classification of esophageal cancer, 10th edition: part I. Esophagus 2009, 6:1–25
19. Japan Esophageal Society: Japanese classification of esophageal cancer, 10th edition: parts II and III. Esophagus 2009, 6:71–94
20. Sobin LH, Gospodarowicz MK, Wittekind C: TNM Classification of Malignant Tumours. ed 7. Hoboken, NJ, John Wiley & Sons, 2011
21. Shigeoka M, Urakawa N, Nakamura T, Nishio M, Watajima T, Kuroda D, Komori T, Kakeji Y, Semba S, Yokozaki H: Tumor associated macrophage expressing CD204 is associated with tumor aggressiveness of esophageal squamous cell carcinoma. Cancer Sci 2013, 104:1112–1119
22. van Rooyen BA, Schafer G, Leaner VD, Parker MI: Tumour cells down-regulate CCN2 gene expression in co-cultured fibroblasts in a Smad7- and ERK-dependent manner. Cell Commun Signal 2013, 11:75
23. Tarasiuk O, Ballarini E, Donzelli E, Rodriguez-Menendez V, Bossi M, Cavaletti G, Scuteri A: Making connections: mesenchymal stem cells manifold ways to interact with neurons. Int J Mol Sci 2022, 23:5791
24. Jo SH, Heo WH, Son HY, Quan M, Hong BS, Kim JH, Lee HB, Han W, Park Y, Lee DS, Kwon NH, Park MC, Chae J, Kim JI, Noh DY, Moon HG: S100A8/A9 mediate the reprograming of normal mammary epithelial cells induced by dynamic cell-cell interactions with adjacent breast cancer cells. Sci Rep 2021, 11:1337
25. Arrigoni C, De Luca P, Gilardi M, Previdi S, Broggini M, Moretti M: Direct but not indirect co-culture with osteogenically differentiated human bone marrow stromal cells increases RANKL/OPG ratio in human breast cancer cells generating bone metastases. Mol Cancer 2014, 13:238
26. Fujita H, Ohuchida K, Mizumoto K, Egami T, Miyoshi K, Moriyama T, Cui L, Yu J, Zhao M, Manabe T, Tanaka M: Tumor-stromal interactions with direct cell contacts enhance proliferation of human pancreatic carcinoma cells. Cancer Sci 2009, 100:2309–2317
27. Miyazaki Y, Oda T, Mori N, Kida YS: Adipose-derived mesenchymal stem cells differentiate into pancreatic cancer-associated fibroblasts in vitro. FEBS Open Bio 2020, 10:2268–2281
28. Suzuki S, Sato M, Senoo H, Ishikawa K: Direct cell-cell interaction enhances pro-MMP-2 production and activation in co-culture of laryngeal cancer cells and fibroblasts: involvement of EMMPRIN and MT1-MMP. Exp Cell Res 2004, 293:259–266
29. Semba S, Kodama Y, Ohnuma K, Mizuuchi E, Masuda R, Yashiro M, Hirakawa K, Yokozaki H: Direct cancer-stromal interaction increases fibroblast proliferation and enhances invasive properties of scirrhous-type gastric carcinoma cells. Br J Cancer 2009, 101:1365–1373
30. Corona A, Blobe GC: The role of the extracellular matrix protein TGFBI in cancer. Cell Signal 2021, 84:110028

31. Thapa N, Lee BH, Kim IS: TGFBIp/betaig-h3 protein: a versatile matrix molecule induced by TGF-beta. Int J Biochem Cell Biol 2007, 39:2183−2194
32. Ween MP, Oehler MK, Ricciardelli C: Transforming growth factor-beta-induced protein (TGFBI)/(betaig-H3): a matrix protein with dual functions in ovarian cancer. Int J Mol Sci 2012, 13: 10461−10477
33. Qin X, Yan M, Zhang J, Wang X, Shen Z, Lv Z, Li Z, Wei W, Chen W: TGFbeta3-mediated induction of periostin facilitates head and neck cancer growth and is associated with metastasis. Sci Rep 2016, 6:20587
34. Yue H, Li W, Chen R, Wang J, Lu X, Li J: Stromal POSTN induced by TGF-beta1 facilitates the migration and invasion of ovarian cancer. Gynecol Oncol 2021, 160:530−538
35. Ozawa D, Yokobori T, Sohda M, Sakai M, Hara K, Honjo H, Kato H, Miyazaki T, Kuwano H: TGFBI expression in cancer stromal cells is associated with poor prognosis and hematogenous recurrence in esophageal squamous cell carcinoma. Ann Surg Oncol 2016, 23: 282−289
36. Suzuki M, Yokobori T, Gombodorj N, Yashiro M, Turtoi A, Handa T, Ogata K, Oyama T, Shirabe K, Kuwano H: High stromal transforming growth factor beta-induced expression is a novel marker of progression and poor prognosis in gastric cancer. J Surg Oncol 2018, 118:966−974
37. Zhang Y, Wen G, Shao G, Wang C, Lin C, Fang H, Balajee AS, Bhagat G, Hei TK, Zhao Y: TGFBI deficiency predisposes mice to spontaneous tumor development. Cancer Res 2009, 69:37−44
38. Wen G, Partridge MA, Li B, Hong M, Liao W, Cheng SK, Zhao Y, Calaf GM, Liu T, Zhou J, Zhang Z, Hei TK: TGFBI expression reduces in vitro and in vivo metastatic potential of lung and breast tumor cells. Cancer Lett 2011, 308:23−32
39. Hung MS, Chen IC, You L, Jablons DM, Li YC, Mao JH, Xu Z, Hsieh MJ, Lin YC, Yang CT, Liu ST, Tsai YH: Knockdown of Cul4A increases chemosensitivity to gemcitabine through upregulation of TGFBI in lung cancer cells. Oncol Rep 2015, 34: 3187−3195
40. Irigoyen M, Pajares MJ, Agorreta J, Ponz-Sarvise M, Salvo E, Lozano MD, Pio R, Gil-Bazo I, Rouzaut A: TGFBI expression is associated with a better response to chemotherapy in NSCLC. Mol Cancer 2010, 9:130
41. Gonzalez-Gonzalez L, Alonso J, Periostin: A matricellular protein with multiple functions in cancer development and progression. Front Oncol 2018, 8:225
42. Kim CJ, Yoshioka N, Tambe Y, Kushima R, Okada Y, Inoue H: Periostin is down-regulated in high grade human bladder cancers and suppresses in vitro cell invasiveness and in vivo metastasis of cancer cells. Int J Cancer 2005, 117:51−58
43. Yoshioka N, Fuji S, Shimakage M, Kodama K, Hakura A, Yutsudo M, Inoue H, Nojima H: Suppression of anchorage-independent growth of human cancer cell lines by the TRIF52/periostin/OSF-2 gene. Exp Cell Res 2002, 279:91−99
44. Ratajczak-Wielgomas K, Kmiecik A, Grzegrzolka J, Piotrowska A, Gomulkiewicz A, Partynska A, Pawelczyk K, Nowinska K, Podhorska-Okolow M, Dziegiel P: Prognostic significance of stromal periostin expression in non-small cell lung cancer. Int J Mol Sci 2020, 21:7025
45. Hu WW, Chen PC, Chen JM, Wu YM, Liu PY, Lu CH, Lin YF, Tang CH, Chao CC: Periostin promotes epithelial-mesenchymal transition via the MAPK/miR-381 axis in lung cancer. Oncotarget 2017, 8:62248−62260
46. Lee YJ, Kim IS, Park SA, Kim Y, Lee JE, Noh DY, Kim KT, Ryu SH, Suh PG: Periostin-binding DNA aptamer inhibits breast cancer growth and metastasis. Mol Ther 2013, 21:1004−1013
47. Contie S, Voorzanger-Rousselot N, Litvin J, Clezardin P, Garnero P: Increased expression and serum levels of the stromal cell-secreted protein periostin in breast cancer bone metastases. Int J Cancer 2011, 128:352−360
48. Li Z, Zhang X, Yang Y, Yang S, Dong Z, Du L, Wang L, Wang C: Periostin expression and its prognostic value for colorectal cancer. Int J Mol Sci 2015, 16:12108−12118
49. Bao S, Ouyang G, Bai X, Huang Z, Ma C, Liu M, Shao R, Anderson RM, Rich JN, Wang XF: Periostin potently promotes metastatic growth of colon cancer by augmenting cell survival via the Akt/PKB pathway. Cancer Cell 2004, 5:329−339
50. Baril P, Gangeswaran R, Mahon PC, Caulee K, Kocher HM, Harada T, Zhu M, Kalthoff H, Crnogorac-Jurcevic T, Lemoine NR: Periostin promotes invasiveness and resistance of pancreatic cancer cells to hypoxia-induced cell death: role of the beta4 integrin and the PI3k pathway. Oncogene 2007, 26:2082−2094
51. Ben QW, Jin XL, Liu J, Cai X, Yuan F, Yuan YZ: Periostin, a matrix specific protein, is associated with proliferation and invasion of pancreatic cancer. Oncol Rep 2011, 25:709−716
52. Kudo Y, Ogawa I, Kitajima S, Kitagawa M, Kawai H, Gaffney PM, Miyauchi M, Takata T: Periostin promotes invasion and anchorage-independent growth in the metastatic process of head and neck cancer. Cancer Res 2006, 66:6928−6935
53. Siriwardena BS, Kudo Y, Ogawa I, Kitagawa M, Kitajima S, Hatano H, Tilakaratne WM, Miyauchi M, Takata T: Periostin is frequently overexpressed and enhances invasion and angiogenesis in oral cancer. Br J Cancer 2006, 95:1396−1403
54. Ishibashi Y, Tsujimoto H, Einama T, Mochizuki S, Kouzu K, Nomura S, Ito N, Harada M, Sugasawa H, Shinto E, Kishi Y, Ueno H: Correlation between immunoinflammatory measures and periostin expression in esophageal squamous cell carcinoma: a single-center, retrospective cohort study. Ann Surg Oncol 2021, 28: 1228−1237
55. Wang W, Sun QK, He YF, Ma DC, Xie MR, Ji CS, Hu B: Overexpression of periostin is significantly correlated to the tumor angiogenesis and poor prognosis in patients with esophageal squamous cell carcinoma. Int J Clin Exp Pathol 2014, 7: 593−601
56. Lambert AW, Wong CK, Ozturk S, Papageorgis P, Raghunathan R, Alekseyev Y, Gower AC, Reinhard BM, Abdolmaleky HM, Thiagalingam S: Tumor cell-derived periostin regulates cytokines that maintain breast cancer stem cells. Mol Cancer Res 2016, 14:103−113
57. Yan W, Shao R: Transduction of a mesenchyme-specific gene periostin into 293T cells induces cell invasive activity through epithelial-mesenchymal transformation. J Biol Chem 2006, 281:19700−19708
58. Takada Y, Ye X, Simon S: The integrins. Genome Biol 2007, 8:215
59. Thongchot S, Singsuksawat E, Sumransub N, Pongpaibul A, Trakarnsanga A, Thuwajit P, Thuwajit C: Periostin regulates autophagy through integrin alpha5beta1 or alpha6beta4 and an AKT-dependent pathway in colorectal cancer cell migration. J Cell Mol Med 2020, 24:12421−12432
60. Ishibashi Y, Mochizuki S, Horiuchi K, Tsujimoto H, Kouzu K, Kishi Y, Okada Y, Ueno H: Periostin derived from cancer-associated fibroblasts promotes esophageal squamous cell carcinoma progression via ADAM17 activation. Biochim Biophys Acta Mol Basis Dis 2023, 1869:166669
61. Kwon J, Lee TS, Lee HW, Kang MC, Yoon HJ, Kim JH, Park JH: Integrin alpha 6: a novel therapeutic target in esophageal squamous cell carcinoma. Int J Oncol 2013, 43:1523−1530
62. Lin SC, Liao YC, Chen PM, Yang YY, Wang YH, Tung SL, Chuang CM, Sung YW, Jang TH, Chuang SE, Wang LH: Periostin promotes ovarian cancer metastasis by enhancing M2 macrophages and cancer-associated fibroblasts via integrin-mediated NF-kappaB and TGF-beta2 signaling. J Biomed Sci 2022, 29:109
63. Zhou W, Ke SQ, Huang Z, Flavahan W, Fang X, Paul J, Wu L, Sloan AE, McLendon RE, Li X, Rich JN, Bao S: Periostin secreted by glioblastoma stem cells recruits M2 tumour-associated macrophages and promotes malignant growth. Nat Cell Biol 2015, 17: 170−182
64. Kormann R, Kavvadas P, Placier S, Vandermeersch S, Dorison A, Dussaule JC, Chadjichristos CE, Prakoura N, Chatziantoniou C:

Periostin promotes cell proliferation and macrophage polarization to drive repair after AKI. J Am Soc Nephrol 2020, 31:85−100
65. Yoshida T, Nagaoka T, Nagata Y, Suzuki Y, Tsutsumi T, Kuriyama S, Watanabe J, Togo S, Takahashi F, Matsushita M, Joki Y, Konishi H, Nunomura S, Izuhara K, Conway SJ, Takahashi K: Periostin-related progression of different types of experimental pulmonary hypertension: a role for M2 macrophage and FGF-2 signalling. Respirology 2022, 27:529−538
66. Jia W, Wang W, Ji CS, Niu JY, Lv YJ, Zhou HC, Hu B: Coexpression of periostin and EGFR in patients with esophageal squamous cell carcinoma and their prognostic significance. Onco Targets Ther 2016, 9:5133−5142
67. Zhu M, Saxton RE, Ramos L, Chang DD, Karlan BY, Gasson JC, Slamon DJ: Neutralizing monoclonal antibody to periostin inhibits ovarian tumor growth and metastasis. Mol Cancer Ther 2011, 10: 1500−1508
68. Kyutoku M, Taniyama Y, Katsuragi N, Shimizu H, Kunugiza Y, Iekushi K, Koibuchi N, Sanada F, Oshita Y, Morishita R: Role of periostin in cancer progression and metastasis: inhibition of breast cancer progression and metastasis by anti-periostin antibody in a murine model. Int J Mol Med 2011, 28:181−186
69. Orecchia P, Conte R, Balza E, Castellani P, Borsi L, Zardi L, Mingari MC, Carnemolla B: Identification of a novel cell binding site of periostin involved in tumour growth. Eur J Cancer 2011, 47:2221−2229